MASTER

ACTUARIAL SCIENCE

MASTER´S FINAL WORK

INTERNSHIP REPORT

CLIMATE CHANGE IMPACT ON NON-LIFE INSURANCE LIABILITIES:
 THE RIVER FLOOD CASE

JOSÉ FILIPE GORDO NEVES

OCTOBER - 2022

MASTER
ACTUARIAL SCIENCE

MASTER´S FINAL WORK
INTERNSHIP REPORT

CLIMATE CHANGE IMPACT ON NON-LIFE INSURANCE LIABILITIES: THE RIVER FLOOD CASE

JOSÉ FILIPE GORDO NEVES

SUPERVISION:
CARLA SÁ PEREIRA
CARLOS MIGUEL DOS SANTOS OLIVEIRA

OCTOBER - 2022

ABSTRACT

The climate change effects on the frequency and severity of extreme weather events are proving to be a challenge to insurance companies. Since August 2022, the European Insurance and Occupational Pensions Authority (EIOPA) demands the inclusion of the prospective climate risks that the insurers expect to impact their businesses in the Own Risk and Solvency Assessment Report (ORSA) under the Solvency II directive. This study focuses on the assessment of the effects of climate change on the specific event of river flooding and the consequent impact on the property insurance portfolio of an insurance company in mainland Portugal. The approach is divided into two moments: (i) the determination of the probability of occurrence of flooding events under three climate scenarios (RCP 2.6, 4.5 and 8.5) and for three time periods (2022-2032, 2032-2050, 2050-2100), using the public data from the Copernicus program; (ii) and the estimation of the vulnerability to floods for the different geographical areas, using data from the Environmental, Planning, Investigation and Cartography WebGIS freely available spatial data infrastructure. The probability of occurrence is given by the variation of the joint return period of precipitation and river discharge for future scenarios based on historical data. The joint probability is investigated by fitting the Clayton, Frank and Gumbel copulas to the data where the margins follow mainly Gamma, Weibull and Generalized Pareto distributions. The analysis shows an expected increase in the probability of occurrence of floods under the RCP 2.6 scenario while decreasing for the other scenarios. The classification random forest algorithm is applied to explain the vulnerability of an area to floods based on the historically flooded areas and their geographical characteristics. According to the computed Gini Importance, elevation and slope are the most important characteristics. The product of the probabilities of occurrence, vulnerability to floods and the sum insured of the property portfolio constitutes the measure of risk to which each area is exposed. Each area is identified by the first two digits of the zip code. The zip codes in proximity to the main Portuguese rivers are the ones that experience a greater risk of losses.

KEYWORDS: Climate Change; Floods; Vulnerability; ORSA; Copulas; Random Forest.

RESUMO

Os efeitos das alterações climáticas na frequência e magnitude em eventos climáticos extremos estão a revelar-se um desafio para as companhias de seguros. Desde agosto de 2022, a *European Insurance and Occupational Pensions Authority* (EIOPA) exige a inclusão dos riscos climáticos que as seguradoras esperam que tenham impacto nos seus *Own Risk and Solvency Assessment Report* (ORSA) ao abrigo da Directiva Solvência II. Este estudo centra-se na avaliação dos efeitos das alterações climáticas sobre o evento específico das inundações fluviais e consequente impacto na carteira de seguros de propriedade de uma companhia de seguros em Portugal Continental. A abordagem está dividida em dois momentos: (i) a determinação da probabilidade de ocorrência de inundações em três cenários climáticos (RCP 2.6, 4.5 e 8.5) e por três períodos (2022-2032, 2032-2050, 2050-2100), utilizando os dados públicos do programa Copernicus; (ii) e a estimativa da vulnerabilidade às inundações para as diferentes áreas geográficas, utilizando a infraestrutura de dados espaciais disponíveis gratuitamente na *Environmental, Planning, Investigation and Cartography WebGIS*. A probabilidade de ocorrência é dada pela variação do período de retorno conjunto de precipitação e descarga fluvial para os cenários climáticos futuros, com base nos dados históricos. A probabilidade conjunta foi determinada para as cópulas de Clayton, Frank e Gumbel em que as margens seguem principalmente distribuições Gama, Weibull e Pareto Generalizado. A análise mostra um aumento da probabilidade de ocorrência de cheias no cenário RCP 2.6, enquanto diminui para os outros cenários. O algoritmo de classificação de floresta aleatória é aplicado para explicar a vulnerabilidade de uma área a inundações com base nas áreas históricas inundadas e suas características geográficas. De acordo com a importância de Gini, a elevação e a inclinação são as características mais importantes. O produto das probabilidades de ocorrência, vulnerabilidade a inundações e a soma dos montantes segurado da carteira constitui a medida do risco a que cada área está exposta. Cada área é identificada pelos dois primeiros dígitos do código postal. Os códigos postais na proximidade dos principais rios portugueses são os que apresentam maior risco de perdas.

PALAVRAS-CHAVE: Alterações Climáticas; Cheias; Vulnerabilidade; ORSA; Cópulas; Florestas Aleatória.

CONTENTS

FIGURES AND TABLES

1 INTRODUCTION

Natural disasters are regular consequences of the dynamics of the Earth's systems. Events such as earthquakes, heat waves, hurricanes, floods, volcanic eruptions and others have required individuals and communities throughout history to adapt to avoid losing their peers and the fruits of their daily labor. While some of these events are particularly uncertain, the current IPCC Sixth Assessment Report (IPCC (2022)) acknowledges with an elevated level of confidence that climate change is having a major impact on the frequency and severity of climate-related events such as heat waves, floods and hurricanes, mainly due to human activity. According to the same report, the effects are far-reaching, more severe in the long term, and depend on actions taken by people, governments and businesses to reduce their footprint. Some consequences of such phenomena are loss of biodiversity, especially for more vulnerable ecosystems; water scarcity due to high snow melt rates, low rainfall rates, agriculture, hydropower and consumption; health problems due to heat waves, diseases related to poor food and water quality, and spread of pathogens; and economic damage to cities, towns and infrastructure (IPCC (2022)).

The insurance sector is particularly exposed to these effects as it covers damages that have been increasing in recent decades. According to the Centre for Research on the Epidemiology of Disasters (CRED (2022)), economic losses worldwide in 2021 alone exceeded aggregate losses for the period 2001-2020. Floods were particularly impactful, with 223 events, and with average losses of USD 74.4 billion, primarily due to incidents in Germany and China (CRED (2022)). Accordingly, efforts have been undertaken by the industry and the academic community to predict and assess damage (e.g. Laudan et al (2017)), prevent losses (e.g. Messner & Meyer (2006)), create new products (e.g. Baskot & Stanic (2020)) and appraise the best risk transfer mechanisms (e.g. Franzke (2017)). Indeed, such solutions include approaches such as the one suggested by Turner et al (2014), which focuses on the growing demand for microinsurance for rare flood events, especially among individuals who have suffered losses in previous events. In Europe, the examination of insurance losses advises the consideration of pooled reinsurance purchasing and shared risk for certain clusters of countries like Austria, Portugal and France, where the first two alone require a high amount of capital for loss cover, but

6

together significantly reduce this figure (Prettenthaler et al (2017)). The study of flood characteristics has evolved towards the application of new and more accurate analysis and forecasting methods, helping not only insurers but also governments and businesses (see for example Lee et al (2017) and Vojtek & Vojteková (2019)).

Portugal has been particularly affected by climate change due to its geographical and climatic characteristics (IPCC (2022)). Intense wildfires, prolonged dry spells, strong winds and floods have been the predominant phenomena (Zêzere et al (2006)). Over the last 40 years, weather events have generated damages of about €7.6 billion, but only 9% of these were covered by available insurance contracts (ECO Seguros (2021)). A number of studies have been carried out on flooding in Portugal and the incorporation of climate change. For example, the Portuguese Foundation for Science and Technology, funded in 2010 the DISASTER project which compiles in a historical geographical dataset the hydromorphological phenomena for the period 1865-2010, observing an increase in the frequency of events for the Lisbon, Coimbra and Porto areas (Carvalho et al (2014)). Da Cunha et al (2007) compiles data from six climate models to perform the forecasts of temperature, precipitation and runoff, for the years 2050 and 2100, finding that during the periods of spring, autumn and summer there is a reduction in the value of runoff for Portuguese rivers.

The estimation of the impact of these events in the insurance contracts has been recently investigated in Portugal (Leal et al (2022)). This thesis intends to further explore the effects of these natural disasters, namely floods, on a property insurance portfolio of an insurance company amid the increasing effects of climate change (IPCC (2022)).

This study will address this issue in two parts: (i) the estimation of the probability of flood occurrence and (ii) the analysis of the flood vulnerability of the regions where properties are insured. The probability of occurrence of a flood event will be calculated under three climate scenarios, scaled by temperature increase, as reported in van Vuuren et al. (2011) and detailed in Appendix A. The estimate will be made under three periods for this century: short term (2022-2032), medium term (2033-2050), and long term (2050-2100), each compared to historical data (1970-2005). Precipitation is the main factor influencing the volume of water flowing through the riverbed and heavy precipitation is expected in Europe under climate change (Seneviratne et al. (2021)). Therefore, the

relationship between precipitation and river discharge will enable the recognition of the levels of both variables which may constitute a flood. Despite variations in probability, the vulnerability of each geographical area depends on hydrological and soil characteristics. From Jacinto et al. (2015) approach, features such as distance to the river, slope, elevation, land use and permeability are going to allow the classification of territories by flood susceptibility. Due to its high accuracy and the extent of the data considered (Breiman (2001)), the random forest algorithm will be the method applied for categorization. The fitting of the distributions and the application of the random forest algorithm were performed in R.

The outline of this thesis is as follows. In Chapter 2, we present the framework and regulations in force and anticipated to be applied to insurance companies regarding climate change. In Chapter 3, the climate change scenarios are introduced based on existing literature, the available data for estimating their effects is described and methods for predicting their impact on flood frequency are presented. Afterwards, in Chapter 4, the vulnerability to river overflow of the different geographical areas of Portugal is investigated, on the basis of the physical characteristics of the region. In Chapter 5, the flood risk related to the amounts insured in specific regions of mainland Portugal for a given insurance company is calculated. The conclusions of this study are set out in Chapter 6.

2   SOLVENCY II AND CLIMATE CHANGE

The Solvency II Directive was introduced in 2009 and became fully applicable on January 1st, 2016. It aims to provide a harmonised, sound, and robust framework for insurance firms in the European Union (EU). Such framework lays on three pillars. Pillar I regards the quantitative requirements for the valuation of assets and liabilities, mainly the methods for calculation of capital requirements and establishment of the eligible own funds to cover such capital requirements. Pillar II concerns the risk management and governance systems. Pillar III addresses the supervisory reporting and public disclosure (European Parliament, 2009). The European Insurance and Occupational Pensions Authority (EIOPA) is responsible for the design of such directives and regulation, not only at EU level, but also at a national level, along with their review according to the sector and overall economic status (European Parliament, 2009). The first amendments were performed on March 8th, 2019, with the objective of promoting the investment on EU scale, for small and medium size companies, and target market deficiencies, through changes in the calculation of certain risks (European Parliament, 2019). The increased significance of events such as windstorms, earthquakes, floods, hail and subsidence were considered due to some contractual policy conditions and early climate change awareness (European Parliament, 2019).

Driven by the COVID-19 crisis and the objectives set by the European Green Deal in 2020, a new revision has been suggested by EIOPA to maintain a sound solvency position and allow for long-term investments that prioritize environmental, social and governance factors. The changes include: (1) a modification of the risk-free discount rate, (2) a new approach to calculate the volatility adjustment, (3) the change in interest rate shocks and their correlation with other market risks, (4) the reduction of the risk margin through the change in the cost of capital charge, and (5) the inclusion of climate change scenarios in the Own Risk and Solvency Assessment (ORSA) (EIOPA, 2019).

2.1 Own Risk and Solvency Assessment

The ORSA specifies how the insurer should meet its future solvency needs in line with: (1) its current business and risk profile, (2) the outlined strategy for the company to achieve its management objectives and (3) the economic, social and environmental context in which it operates. The ORSA policy should establish the rules for assessing the consequences of the business strategy and its risks. The latter include: (i) the risk tolerance limits, (ii) the timing and frequency of reporting, (iii) the stress and sensitivity tests used for the solvency and financial structure of the company and (iv) information on the quality of the data used for such assessment (Prudential Regulation Authority, 2016).

The inclusion of climate change in the calculation of capital requirements is undertaken partially in the standard formula under life, health and non-life risks and for one year. However, the impact of climate change is only observable considering the medium and long-term outlook. In contrast, the current temporal structure of ORSA only considers projections over a maximum timeframe of 5 years. Therefore, consistent with the approach adopted by the Intergovernmental Panel on Climate Change (IPCC), ORSA can consider three periods depending on their temporal proximity: short-term (5-10 years), mid-term (up to mid-century) and long-term (up to the end of the century) (EIOPA (2022)).

2.2 Climate Change Risks

Climate variability is a natural consequence of the Earth's rotation and orbit, feedbacks on the climate system and random fluctuations on physical and chemical factors. However, human influence on climate is now more certain than ever, with numerous studies and people's experiences proving that the frequency and severity of climate phenomenon is increasing (IPCC (2022)). Accordingly, efforts have been made by governments, businesses and citizens to reduce the impact of human activities on the environment (IPCC (2022)). Climate change risks constitute the elements of climate change that introduce uncertainty into insurance companies' assumptions when assessing the materiality of such risks to their business (EIOPA (2022)). Consistent with the nature of the risks, they can be classified into 2 types: transition risks and physical risks.

Transition risk is one of the drivers of climate risk comprising the uncertainty associated with the efforts of governments and businesses to move the economy towards

decarbonization and resilience to climate change. This includes political, legal, technological, market and reputational risks (EIOPA (2021)). Greenhouse gas emissions-related businesses are especially susceptible to this type of risk and insurers should be especially cautious in assessing the impact of transition on assets and liabilities. Deterioration of investor and other counterparty confidence in carbon-intensive companies leads to loss of value of their assets and financing difficulties as their stakeholders shift to greener activities (EIOPA (2021)). On the liability side, underwriting insurance to 'brown' companies might lead to impaired trust in the insurer and in the expected value of claims, driving up premiums as well.

The predominant part of climate change risk is physical risk. These risks translate the physical effects of the associated extreme events in terms of property damage, business interruption, decreased profitability and increased mortality (EIOPA (2021)). Physical risks are classified into 2 groups: (1) acute risks, related to one-time events such as storms, floods, fires and droughts which cause high damage and temporary disruption of activities; (2) chronic risks related to long-term exposure to climate change, such as general temperature increase, water scarcity, loss of biodiversity, etc. (EIOPA (2021)). Due to the potential magnitude of the damages, physical risks are those of greatest concern to supervisors and whose impact is projected to increase (EIOPA (2022)).

In this work, we will focus on the assessment of the physical impacts of climate change on flooding for mainland Portugal and its effects on a property portfolio of an insurance company.

3   FLOOD FREQUENCY PREDICTION

Different approaches to the effect of climate change on the flood frequency and severity trends identification are observed for both historical data and projections of river flow and/or rainfall behaviour. Madsen H. et al. (2014) revisit studies on flood frequency in Europe and conclude a general increase in extreme precipitation and flows in some river basins. Through methods such as linear regression, positive trends are observed, and the effects of climate change are expected to have an even greater impact on this trend. For future projections, the predominant approach focuses on the calculation of the return period. The return period of a given event is given by the average time between two

consecutive occurrences of the same event (Gumbel (1941)). A flood occurs when the river discharge exceeds a certain threshold. Hence, the flood return period will be the mean time between two instances when this threshold is exceeded. Anandalekshmi et al (2018) employ return periods to examine the effect of extreme rainfall on reservoir storage during three periods: 2005-2010, 2010-2015 and 2015-2018. The observed return periods were 96, 102 and 289 years, demonstrating a decrease in the impact of extreme rainfall on reservoir overflow, mainly because of the effectiveness of controlled release of excess water.

Despite the empirical nature of flood data, fitting continuous distributions is a commonly used approach to better capture the dynamics of the variables being studied (Singh (1998), Saf (2009) and Yin et al. (2018)). The adjustment methods employed are the method of moments, the maximum likelihood estimator, the maximum entropy principle as proposed by Singh (1998) or the L-moments method (Saf (2009)). The most commonly used distributions include Gamma, Gumbel, Extreme Value, Pearson III, Log-Pearson III, Lognormal and Generalised Pareto. The goodness of fit is usually evaluated using the mean squared error criterion and Akaike information (e.g. Yin et al. (2018)) or via conduction of tests such as Kolmogorov-Smirnov test, Chi-square test (e.g. Karmakar and Simonovic (2009)).

The evaluated factors include precipitation, river flow, duration, volume and intensity of the flood. The identification of the distribution that best represents the behaviour of each variable and, thereafter, of the joint distribution of these variables, provides a better description of the phenomenon. For example, Correia (1987) looked at the three flood characteristics: duration, volume, and flood peak, for a set of Portuguese rivers located in the northern part of the country. Following the fitting of a set of distributions, Correia concludes that the assumption of the independence between rivers for the main factors that influence the river volume, even if they are connected, is applicable to most Portuguese rivers. These assumptions will also be considered in the present study.

The individual evaluation of the variables being investigated is possible (e.g. Gumbel (1971)), however these variables are dependent on each other. Therefore, joint analysis is an appropriate approach. The interaction between variables was tackled by Yue (2001), who evaluates the behavior of these same characteristics for the time series of river flow

in the Harracana basin, Quebec, Canada. The Gumbel Logistic Model, a joint cumulative function of two variables assumed to follow a Gumbel-type marginal distribution, was considered. Given the complexity of estimating a joint probability function, Salvadori and De Michele (2004) gives an intensive review of the concept of copula, the different forms of presenting the return period and its applications in different studies for pairs of flood features. By accounting for only two features, their graphical presentation is possible, thus bivariate analysis is prevalent in the literature. Nevertheless, the capabilities of copulas allow for the inclusion of a larger number of features. For example, Zhang and Singh (2007) proposed a trivariate Gumbel-Hougaard copula. The copula parameters are estimated using the maximum pseudo-probability estimator, the maximum likelihood estimator, and the method of moments (e.g., Klein et al. (2010)). The goodness-of-fit measures are in the multivariate case similar to those used in the univariate case (Karmakar and Simonovic (2009), Zhang and Singh (2007)).

The choice of the appropriate copula is a delicate process given the spatial constraints of each and the suitability in terms of tail dependence, as highlighted by Chowdhary et all (2011). For the universe of 29 copulas, the admissibility intervals for Kendall's tau and tail dependence coefficients were analyzed and concluded that the Ali-Mikhail-Haq, Clayton, Frank, Galambos, and Gumbel-Hougaard copulas would be the best fit. Some novel approaches, such as the one proposed by Wen et al. (2019), extend the copula concept by introducing a time-varying term where the parameters of the marginal distributions and the copula itself are described as one dependent variable of a linear regression.

To include the effect of climate change, sophisticated climate and hydrological models can be used to project the different factors, including global/regional circulation models and a range of climate scenarios (Yin et al. (2018)).

In this thesis, the variable pair of daily mean river discharge[1] and daily mean precipitation data is considered. Historical data is outlined, and future projections for three climate scenarios are elaborated. In the following section, the mathematical framework for the study of marginal and joint variables is presented, as well as the study of return period adjustment.

---

[1] volume rate of water flow transported through a given river cross-sectional area (Berg et al. (2021b))

3.1 Copulas and Return Period

Let $U_1, U_2, \ldots, U_d$ be continuous random variables uniformly distributed over the interval [0,1]. The copula $C: [0,1]^d \rightarrow [0,1]$ is a joint distribution function such that (see for instance Nelsen (2006)):

$$C(u_1, u_2, \ldots, u_d) = \text{Pr}\,(U_1 \leq u_1, U_2 \leq u_2, \ldots, U_d \leq u_d)$$

Also, let $X_1, X_2, \ldots, X_d$ be the marginal continuous random variables with distribution functions $F_1, F_2, \ldots, F_d$. Then, by Sklar's theorem, for any distribution function H, there exists a copula C such that (see for instance Nelsen (2006)):

$$
\begin{aligned}
H(x_1, x_2, \ldots, x_d) &= \text{Pr}(X_1 \leq x_1, X_2 \leq x_2, \ldots, X_d \leq x_d) \\
&= \text{Pr}(F_1(X_1) \leq F_1(x_1), F_2(X_2) \leq F_2(x_2), \ldots, F_d(X_d) \leq F(x_d)) \\
&= \text{Pr}(U_1 \leq F_1(x_1), U_2 \leq F(x_2), \ldots, U_d \leq F(x_d)) \\
&= C(u_1, u_2, \ldots, u_d)
\end{aligned}
$$

The copulas to be considered in this study are part of a class called Archimedean copulas. Let $\varphi: I \rightarrow [0, +\infty]$ be a strictly decreasing continuous function such that $\varphi(1) = 0$, where I is the domain of φ. Let $\varphi^{[-1]}$ be the pseudo-inverse function of φ defined in Equation 1.

$$\varphi^{[-1]}(t) = \begin{cases} \varphi^{-1}(t), 0 \leq t \leq \varphi(0) \\ 0, \varphi(0) \leq t \leq +\infty \end{cases} \tag{1}$$

Then an Archimedean copula $C: I^d \rightarrow I$ is defined as (Nelsen (2006)):

$$C(u_1, u_2, \ldots, u_d) = \varphi^{[-1]}(\varphi(u_1) + \varphi(u_2) + \cdots + \varphi(u_d))$$

Where φ is denoted the generator function. The generator functions for the copulas applied to this work are presented in Appendix B. In this study, the analysis will focus on the Clayton, Frank, and Gumbel copulas.

The parameters are estimated by means of the Inverse Kendall's Tau method, which like the method of moments, considers this dependence measure as consistent estimator for copula parameter (Nelsen (2006)). For this method, the theoretical Inverse Kendall's Tau for the copula of the population is given by the one of a sample of such population. Let (X_1, X_2) e (X_1^*, X_2^*) be the pairs of random variables with the same marginals $F_1(x_1)$ and $F_2(x_2)$, the Kendall's Tau correlation coefficient measures the level of correlation between these pairs of variables:

$$\tau_k(X_1, X_2) = \Pr[(X_1 - X_1^*)(X_2 - X_2^*) > 0] - \Pr[(X_1 - X_1^*)(X_2 - X_2^*) < 0]$$
$$= E\left[sign\left((X_1 - X_1^*)(X_2 - X_2^*)\right)\right]$$
$$= 4 \int_0^1 \int_0^1 C(u, v)\, dC(u, v) - 1$$

The quality of adjustment of the copula is determined by the Akaike Information Criteria (AIC). The lower the value of the statistic, the better the quality of adjustment. In its copula version, the AIC is described as follows (see for instance Ko et al. (2019)):

$$AIC = 2k - 2 \sum_{i=1}^{n} \ln(c(F_X(x_i), F_Y(y_i)) f_X(x_i) f_Y(y_i))$$

Where c is the copula density function, n is the size of the sample and k is the number of parameters.

One of the methods for copula fitting requires the determination of distribution function of the marginals, which can change the dynamics of the interaction between the variables under study. For instance, the prior analysis of the tail behaviour of hydrological variables such as river discharge allows for the evaluation of the potential magnitude of flooding events in a certain area. In accordance with the literature, the distributions to be fitted to individual precipitation and river discharge are as outlined in Appendix C, where location, scale, and shape are the parameters of the functions.

To adjust the marginals, traditional methods are used: the method of moments, the maximum likelihood estimator, and the L-moments method, derived from weighted

moments in which, instead of considering the order statistics individually, linear combinations of these statistics are considered (Saf (2009)).

The quality of fit is measured by four statistics: Akaike Information Criterion, Chi-Square Test, Cramer von Mises and Kolmogorov-Smirnov, are described in Table I. In all cases, the lower the value of the statistic, the better the fit of the distribution:

Table I: Margins' Goodness-of-Fit Statistics

Goodness-of-fit Tests	Statistic	Distribution
Akaike Information Criterion	$AIC = 2k - 2\sum_{i=1}^{n} \ln f(x_i)$	
Chi-square Test	$X^2 = \sum_{i=1}^{n} \frac{(x_i - np_i)^2}{np_i}$	$\chi^2_{(n-1)}$
Cramer von Mises	$T = \frac{1}{12n} + \sum_{i=1}^{n} \left(\frac{2i-1}{2n} - F(x_i)\right)^2$	$\omega_n^2 = n \int_{-\infty}^{\infty} \{F_n(x) - F(x)\}^2 \, dF(x)$
Kolmogorov-Smirnov	$D_n = \sup_x |F_n(x) - F(x)|$	$\sqrt{n}D_n \to \sup_x |B(F(x))|$

n: sample size, k: number of parameters estimated, $f(x)$: probability function, p_i: expected probability, $F(x)$: cumulative distribution function, $F_n(x)$: empirical distribution function, B(t): Brownian bridge

Note that despite the test results, graphical observation of the distribution against the empirical distribution and expert opinion may suggest a different adjustment from the one statistically accepted.

Let $F(x)$ be the cumulative distribution function of the random variable X, the return period corresponds to the average number of trials, $T(x)$, that must be made for the realization of X to be greater than or equal to a given value x. Let μ_T be the time unit of the considered observations, which for annual values is 1 (Salvadori and De Michele (2004), Gumbel (1941)), then:

$$T(x) = \frac{\mu_T}{1 - F(x)}$$

Each variable has a different behavior described by its cumulative distribution function. So individually, the return periods will be different. In the bivariate case, the interaction between the two variables is considered to change the pattern of the return period. Joint return periods, modeled by copulas, describe the joint dependence of the characteristics of interest (Salvadori and De Michele (2004), Anandalekshmi et al. (2019)). Two types of joint return periods are considered, based on the realizations of X and Y. In the AND case ($\wedge$), the return period is given by the average number of trials between two events where X exceeds a certain threshold and, at the same time, Y exceeds a threshold befitting Y's behavior. For example, a scenario of high precipitation and high river discharge is more prone to flooding, since precipitation levels are the main driver of river overflow (Salvadori and De Michele (2004)). The joint return period AND is presented in Equation 2:

$$T_{X \wedge Y}(x, y) = \frac{\mu_T}{\Pr (X > x \wedge Y > y)} = \frac{\mu_T}{1 - [F_X(x) + F_Y(y) - C(F_X(x), F_Y(y))]} \quad (2)$$

In the OR case ($\vee$), the return period is calculated between two events where X or Y exceed the respective thresholds. Precipitation and river discharge alone do not set up a river flood situation since high precipitation levels alone cannot cause flooding due to dams and other flood prevention mechanisms (Anandalekshmi et al. (2019)). This case is applied to other extreme weather events like storm surges (Salvadori and De Michele (2004)). The joint return period OR is presented in Equation 3:

$$T_{X \vee Y}(x, y) = \frac{\mu_T}{\Pr (X > x \vee Y > y)} = \frac{\mu_T}{1 - C(F_X(x), F_y(y))} \quad (3)$$

Thus, the assessment of the joint behavior of the variables under study is important when modeling flood risk. This study will focus on the joint return period AND, since a combined scenario of extreme precipitation and high river discharge is more prone to flooding.

3.2   Data

In this section, we will describe the data used to assess the probability of fluvial flood occurrence for three climatic scenarios and for three time periods. The data was collected from the Copernicus program for the mainland Portugal area and confirmed with data from the the *Sistema Nacional de Informação de Recursos Hídricos* (SNIRH).

The Copernicus program, developed by the European Union in partnership with the other European agencies, seeks to process and analyze real-time data from atmosphere, land and oceans through dedicated satellite systems and local meteorological and hydrological stations (Berg et al. (2021a), Berg et al. (2021b)). Towards the analysis of flood phenomena in Europe, Copernicus provides historical data (1971-2005) and future projections (2006-2100), according to three climate scenarios, for precipitation, measured in millimeters per day and river discharge, the volume of water flowing through the channel of a river, measured in cubic meters per second.

Until the IPCC Fourth Assessment Report (AR4), the literature included about 300 climate scenarios, considering or not the possibility of stabilisation of emissions (Moss et al. (2008)), so the IPCC decided to compile the information from all these studies into four trajectories according to the emission and concentration of greenhouse gases and other pollutants in the atmosphere and land use: the Representative Concentration Pathways (RCPs). Details of emission quantities and other characteristics can be found in Appendix A. Following van Vuuren et al. (2011), of these, the three scenarios considered will be (1) RCP 2.6, representing a mitigation scenario, which leads to a decrease in global temperature; (2) RCP 4.5, a medium stabilisation development; and (3) RCP 8.5, a very high emissions scenario, corresponding to continued fossil fuel consumption and no cooperation between countries.

The data provided by Copernicus extends over mainland Portugal with a resolution of 5 km, according to a Lambert azimuthal and rotating grid (Figure 1). A set of 3550 points is available, combining the Hadley Centre Global Environment Model version 2

(HadGEM2-ES), developed by the Met Office, and the local information obtained by the RACMO version 2.2e (RACMO22E), from the Koninklijk Nederlands Meteorologisch Instituut (KNMI), duly corrected for bias.

Figure 1 – Copernicus grid points

The precipitation is the deposition of water in the form of rain, snow, ice, or hail, expressed in kilograms per square meter per second ($kg\ m^{-2}s^{-1}$) (Berg et al. (2021a)). However, in most local stations, an instrument called a pluviometer measures the amount of liquid precipitation over a unit area, usually expressed in millimeters per unit of time. On the other hand, historically, snow, ice and hail are not that expressive in the Portuguese territory, therefore the pluviometer units are the ones used hereafter. Considering that one kilogram of rainwater spread over one square meter of surface is one millimeter in thickness and that there are 86400 seconds in a day, then $1\ kg\ m^{-2}s^{-1}$ is equivalent to 86400 mm/day. Therefore, all precipitation data multiplies by a factor of 86400. The river discharge units are in m^3s^{-1} and represent the volume rate of water flow transported through a given cross-sectional area per second (Berg et al. (2021b)). Further details on the data are presented in Appendix B.

According to the expectations of the ORSA reports for coming years, the three climate scenarios are divided by three periods: short term (2022-2032), medium term (2032-2050) and long term (2050-2100). Recognizing the best distribution for each grid point is essential to obtain a proper fit of the copula and subsequent determination of the joint return period. For each statistical test presented in section 3.1, the two distributions with the lowest statistical value are selected across all estimation methods and from these the one with the best fit is selected. For precipitation, the best distributions are primarily the Gamma, Generalized Logistic and Weibull. For river discharge, apart from the Gamma and Weibull distributions, the Generalized Pareto is one that presents the best fit.

Among the parameter estimation methods, the L-moments method performs better for selected best distributions. Figure 2 shows the fitting of the three methods compared to the empirical distribution function for one of the historical data points with coordinates (8.63ºW, 39.29ºN) corresponding to a grid point near the Tejo river:
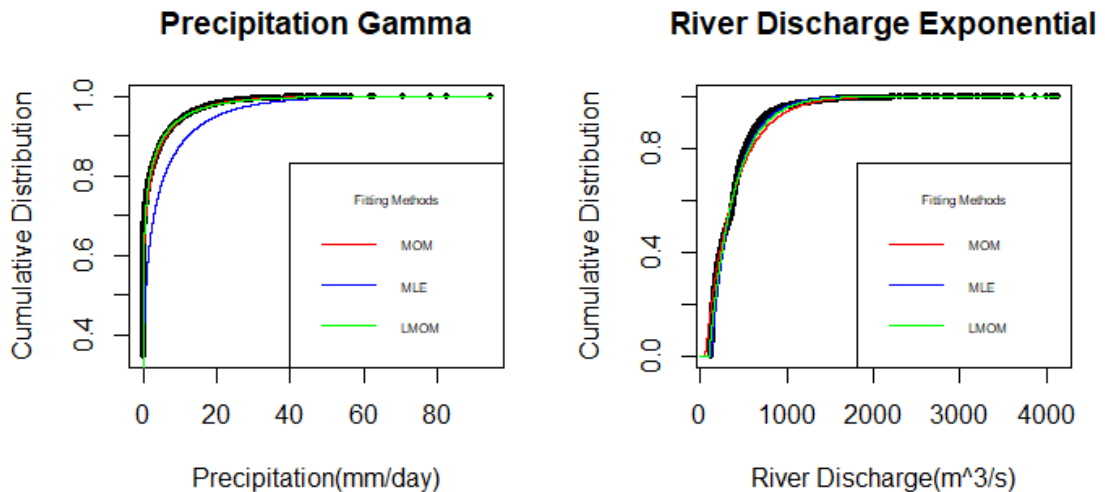
Figure 2 – Distribution functions for the three estimation methods: method-of-moments, maximum likelihood estimator and L-moments

After recognizing the best distributions and its parameters for both precipitation and river discharge, the copula functions must be adjusted. The best copula is identified by

20

means of the Akaike Information Criteria. The best fitting copula out of the three considered for most of the grid points was the Gumbel copula. The Gumbel copula is characterized by having upper tail dependence, i.e, when one of the variables attains large values, the other has a high probability of presenting a large value as well. In the context of flooding, this property is desirable since it expresses a positive correlation between the variables and, especially, in a combined scenario of heavy precipitation and high river discharges, the one that causes floods. The empirical and fitted copulas for the grid point of coordinates (8.63ºW, 39.29ºN) are presented in Figure 3:

Clayton Copula Distribution Function
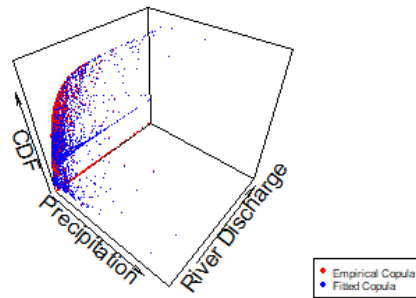
Figure 3 – Empirical and Fitted Copulas

After determining the best fitting copula, we proceed to the calculation of the joint *AND* periods for the considered climate scenarios and periods. Recalling the concept of return period, the higher the return period, the less likely is for the variable being tested to exceed the given threshold. For example, a precipitation value with 100-year return period means that the probability that the threshold is exceeded is of 1%. This does not mean that such precipitation values will be observed in periods of 100 years. They may be observed twice in the same year, but with reduced probability. Therefore, the combination of precipitation and river discharge to cause a flooding event is expected to have a high return period.

In line with the approaches found in the literature and the properties of the return period, the following procedure was considered to determine the variation on potential flood events:

(1) Calculate the joint return period *AND* for the historical data. For each grid point, consider the best fitting copula determined before. Since the copula is a function of the distributions functions and their domain is in the interval [0,1], then by considering the combinations of values in this range, a matrix of the possible return periods is obtained. Computationally, vectors of length 1000 out of this interval are considered.

(2) Inspect the pairs of values with the following return periods: 100, 1000 and 10000. Notice that a one million return period implies that the values for precipitation and river discharge, together, expected to exceed the threshold one out of one million times.

(3) Determine the precipitation and river discharge quantiles for the values determined in step 2 by using the best fitted margins for each grid point.

(4) For the different climate scenarios and time periods, calculate the return period for the quantiles determined in step 3.

The inverse of the difference between the return periods obtained for the different pairs (climate scenario, time period) for the historical data quantiles and the respective return period considered in the calculation of such quantiles (100, 1000 and 10000 years) gives the probability of occurrence of river flooding for each point in the grid.

For example, a decrease in the return period suggests an increase in the probability of occurrence of the precipitation and river discharge values relative to a historical exceedance probability of 1%, 0.01% and 0.0001%. Figure 4 classifies the grid points according to the sign of the return period variation. The variations that are infinite are removed from the analysis since they are negligible (the exceedance probability is 0%):
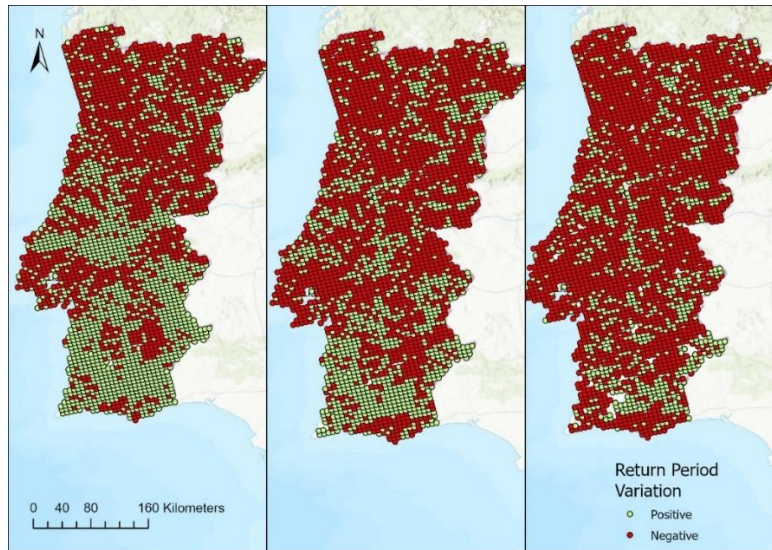
Figure 4 – Return Period Variation for 100-year, 1000-year and 10000-year historical precipitation and river discharge under the RCP 2.6 short term scenario

4 ESTIMATING THE VULNERABILITY TO FLOODS IN PORTUGAL

The extent of damage caused by these phenomena is heterogeneous, so the distribution of benefits payable to policyholders and the insurance premium collected can be adjusted by the insurer to minimize their losses. The degree of heterogeneity of damage depends on the vulnerability of the geographical area. The definition of vulnerability to natural disasters varies between authors and organizations. Attempts have been made to incorporate all the indicators that can influence the harmful consequences of disasters and it depends on (1) the type of study, (2) the objective of the results to be obtained, (3) the type of hazard, (4) the geographical area to be considered and (5) the time horizon (Barroca et al. (2006)).

Blaikie et al. (1994) define vulnerability to hazards as the ability (or inability) of a given population to anticipate, withstand and recover from a natural disaster and all events or series of events associated with it. Adger (2006) defines it as the susceptibility to environmental and social change due to inability to adapt and describes the linkages between humans and the environment and our role in managing such interactions. The above concepts of vulnerability are relatively vague as they cover a range of indicators that may be inadequate. Numerous authors have therefore sought to define vulnerability as a function of other, simpler concepts (Adger (2006), Rehman et al. (2019)). UNESCO,

in its flood vulnerability index, whose purpose is to facilitate decision making for policy makers and investors, sets out the following equation in which the relationship between the concepts can be observed (Rehman et al. (2019)):

$$Vulnerability = Exposure + Susceptibility - Resilience$$

In this study, UNESCO's approach will be one to considered. Exposure stands for the people, goods and structures potentially subject to damage due to a natural hazard, which in this thesis is given by the sum insured for each geographical area. Susceptibility is the predisposition of an area to be affected by such hazard, which will be measured by classification of each geographical area, according to its probability to flooding, considering the landscape, soil and waterflow conditions of the area. The procedure is detailed in the next sections. Resilience is the capacity of a system to resist the hazard and return to an acceptable state of organization and functioning (Rehman et al. (2019)), which will not be considered in this study. Several methods are available for the measurement of these concepts (e.g., Kazakis et al. (2015) and Samanta et al. (2018)) and some will be described in the next section.

According to the nature of the variables considered, vulnerability to floods is divided in four types (Chan et al. (2021)):

(1) **Physical vulnerability** poses the natural structures and indicators that influence the flow of fluids such as air and water towards an area. Factors such as elevation, proximity to river, the normalized differential vegetation index, slope, flow accumulation and permeability are considered. The authors conclude that the proximity to the river, elevation and slope are the most crucial factors (Vojtek and Vojteková (2019))

(2) **Environmental vulnerability** encompasses the ecological footprint that these events cause in the ecosystems and the potential of the system for regeneration depending on characteristics such as the soil, species that inhabit the area and the level of organization in terms of the food chain (Williams and Kapustka (2000)).

(3) **Social vulnerability** addresses the impacts and ability of the individuals and communities to overcome the damages imposed by a natural disaster. The factors

that influence such ability include socioeconomic status, gender, age, commercial and industrial development, employment loss, infrastructures, occupation and others (Boruff et al. (2003)).

(4) **Economic vulnerability** which concentrates on the ability of private and public infrastructures to withstand impacts (Woodruff et al. (2018)). Fatemi et al. (2020) addresses the interaction between physical vulnerability, flood response and adaptability strategies for Dhaka city in Bangladesh considering variables like the main construction material of the roof, walls and floor, the height and age of the building, and the presence of flood protection measures in the building, concluding that older, fragile, and lower buildings experience higher damage.

The data available to proceed to the evaluation of the vulnerability areas to flood in mainland Portugal is mostly related to physical vulnerabilities except for the land use which can be considered an economic vulnerability factor. A further interpretation of the variables used is detailed on chapter 4.2.

4.1 *Measurement Methods*

The identification of flood prone areas is carried out after these events happen which can be hard, costly and time consuming. Therefore, the prior modelling of the vulnerability of each region is a valuable tool for prevention and protection against major damage (Kho et al. (2018)). The models available differ in accuracy, data used, structure and processing time (Shafizadeh-Moghadam et al. (2018)). Each model has its advantages and disadvantages so there is no consensus on which models to choose (Khosravi et al. (2018)). Four approaches to modelling flood can be considered (Olowe (2021)):

(1) **Hydrological approach** refers to models that gather flood and landscape data and through hydrodynamics equations assess the impacts in the several areas, mainly around the river. Despite their accuracy, the data collection can be costly and time consuming. Abdulkareem et al. (2018) review 70 studies conducted for Malaysia, concluding that 60% percent of them applied hydrological models.

(2) **Qualitative approaches** attempt to consider expert knowledge and decision-based techniques to relate independent flood characteristics. The main techniques used are the Analytical Hierarchy Process (AHP) (e.g., Kazakis et al. (2015)),

Technique for Order Preference by Similarity to an Ideal Solution (TOPSIS) (e.g. Lee et al. (2013)), Simple Additive Weighting (SAW), and other multi-decision criteria methods (e.g., Malekian and Azarnivand (2016)).

(3) **Statistical approaches** presume the calculation of statistics which range of values allows for the identification and classification of an area. The most common practices are the frequency ratio (e.g., Samanta et al. (2018)), logistic regression (e.g., Shafapour et al. (2019)), weight of evidence (e.g., Khosravi et al. (2016)) and entropy (e.g., Siahkamari et al. (2018)).

(4) **Machine Learning Methods** are becoming more popular for pattern recognition, prediction, and classification, due to the increase in computational power and the developments in artificial intelligence (Olowe (2021)). There are several algorithms available under the machine learning umbrella which for flood vulnerability include (boosted-)decision trees (e.g., Lee et al. (2017)), support vector machines (SVM) (e.g., Tehrany et al. (2014)), artificial neural network (ANN) (e.g., Falah et al. (2019)), generalized linear models (GLM) (e.g., El-Haddad et al. (2021)) and random forests (RF) (Lee et al. (2017)).

In this study, random forests were considered due to their high accuracy. In the random forest methods estimates are performed variable importance and the substitution of missing values is carried out according to the values in its neighbourhood (Breiman (2001)), which also make this methodology appealing.

4.1.1 Random Forests

The random forest methodology encompasses a group of algorithms where for each random vector generated from the training data, a hierarchical tree structure is applied so that the child nodes are a result of a set of constrains established according to the nature of the variables included in the analysis (Breiman (2001)). Random forests are used for both regression and classification and the general algorithm can be described as follows (Hastie et al. (2009)):

1. For b from 1 to B:

a) Randomly generate one bootstrap sample of size N out of the training data.

b) Grow a random forest, T_b , splitting each node by picking the best variable

or split point out of a set of m variables from the original variables.

(This procedure will be detailed later)

Repeat the process until the minimum node size is reached,

where the minimum node size is 10.

2. Output the forest, i. e. , the group of B trees.

The prediction of a new point using random forests depends on whether they are used for regression analysis or classification, that is, to assess the impact of a set of variables into a dependent variable. In regression analysis, the prediction is given by the average of the values obtained for each tree that presents the same characteristics as the new point. For classification, it is given by the majority vote out of the trees with random vector like the new point (Hastie et al. (2009)).

In the context of flood vulnerability, rather than a binary classification of the areas, the determination of the probability of belonging to each group allows the ranking of the likelihood of such event to happen. Malley et al (2012) propose the estimation of the conditional probability function for a binary outcome by means of machine learning methods, like random forests, which are proved to perform well for non-parametric regressions. Therefore, the classification random forest is first applied and then the expected value of the dependent variable, given the feature vector for the different trees, is determined.

Let Y be the binary variable under study and X the explanatory variables, the conditional probability of the characteristic being observed ($P(Y = 1|X)$) is equivalent to the expected value of Y conditional on X, which is a Bernoulli random variable.

Therefore, the probability estimation problem can be resumed to the following non-parametric regression:

$$\hat{P}(Y = 1) = E(Y|X = x)$$

The consistency of this approach has been proved for the random forest classification by observing the convergence of the mean squared error (MSE) and if the bagging method is used (Malley et al (2012)). According to Breiman (2001), bagging consists in growing a tree by using a new training set from the resampling with replacement of the original dataset and with a random selection of the explanatory features. The error rate on the training set is considered as measure for the quality of the random forest model used (Breiman (2001)). This approach is the one considered in this study.

Since the true probability of flooding is not available and the consistency of the classification random forest has been proved, the Brier score can be used instead as an error quantifier. Let N be the training sample size and y_i the observed dependent variable, then the Brier score (BS) is given by:

$$BS = \frac{1}{n} \sum_{i=1}^{N} (y_i - \hat{P}(Y_i = 1))^2$$

The Brier score is equivalent to the mean squared error but for predicted probabilities. The score's aim is to penalize inaccurate predictions and varies between 0 and 1. For instance, in this study, if for a certain geographical area, the historical indicates that flooding event happened, but the prediction model suggests the opposite, then the expected score for that observation will be high. The lower the score, the better the predictions.

The criteria for splitting the nodes and pruning the tree differs on the type of model and is based on the calculation of the impurity of the nodes. In classification analysis, the misclassification error, Gini importance and cross-entropy are the most used. In this study, the Gini importance is the one considered (Hastie et al. (2009)).

Let (x_i, y_i) be the observations of the variables X and Y and consider a partition of the sample space (x_i, y_i) into M regions $R_1, R_2, \ldots, R_M$. The Gini index $Q_m(T)$ for the tree T and node m is defined as follows (Hastie et al. (2009)):

$$Q_m(T) = \sum_{k=1}^{K} \widehat{p_{mk}}\,(1 - \widehat{p_{mk}})$$

Where $\widehat{p_{mk}}$ is the number of class k observations in node m, with $k \in 1, \ldots, K$, where K the number of classes of the dependent variable considered. Let R_m be a particular region and $I(y_i = k)$ the indicator function which is one when the observed dependent variable is equal to the considered class k:

$$\widehat{p_{mk}} = \sum_{x_i \in R_m} I(y_i = k)$$

This is also used in the assessment of importance of each independent variable. The higher the Gini importance, the more significant is the variable (Hastie et al. (2009)).

4.2 Spatial Datasets

In this section, we present the variables chosen for the classification of the vulnerability to flood of mainland Portugal.

The dependent variable is given by the geographical areas where floods with considerable damage and loss of human lives were historically observed. Therefore, it can be represented as a binary variable and the random forest classification is adequate. The data is available at the Agência Portuguesa do Ambiente (APA) portal and embraces the studies, reports, news and articles on floods, hidrological information and planning out of the *Sistema Nacional de Informação de Recursos Hídricos* (SNIRH).

Regarding the independent variables, these were selected according to the indicators usually considered in the literature and out of the Environmental, Planning, Investigation and Cartography WebGIS (EPIC WebGIS) freely available spatial data infrastructure. The EPIC WebGIS developed as part of the *PTDC/AUR-URB/102578/2008 – National Ecological Network – a proposal of delimitation and regulation* (EPIC WebGIS Portugal (2022)). The datasets considered are the following: current permeability, elevation, and slope. The distance to the river is determined by calculating the distance of the geographical areas to the main rivers and lakes in mainland Portugal. The ArcGIS Pro's tool Euclidean Distance allows for the creation of a spatial dataset with such distances.

The water bodies extent is accessible at the APA portal. The last indicator, the Land Use, is provided by the Direção Geral do Território, in its 2018 Soil Usage and Occupation Cartography. Only elevation and distance to river are continuous variables while the remaining are categorical. Table II summarizes the explanatory variables used in this study (EPIC WebGIS Portugal (2022)):

Table II – Explanatory Variable Details

Explanatory Variable	Description	Scale/ Spatial Resolution	Classification
Elevation	Terrain altitude with respect to the sea level	25m	Continuous Variable
Slope	Degree of inclination of a surface	25 m	From flat areas to very hilly areas, seven classes: 0-3%, 3-5%, 5-8%, 8-12%, 12-16%, 16-25%,> 25%.
Current Permeability	Qualitative assessment of water infiltration capacity of the soil	1:100000	Seven classes: Low, Low to Medium, Medium, High, Very High, Water Plains and Urban Areas
Distance to River	Shortest distance between a water body (river or lake) and spatial pixel	25m	Continuous Variable
Land Use	Cartographic information of the usage and occupation of the soil	20m	10 classes: Artificialized territories, Agriculture, Pastures, Agro-Forestry areas, Forests, Bushland, Open spaces or sparcely vegetated areas, Wetlands and Surface water bodies

4.3   Methodology and Results

The application of the random forest algorithm requires the rasterization[2] of all the datasets for the same resolution and the pixels must match each other. Since the original resolution and pixel positioning is different for the considered datasets, a resampling of the datasets through bilinear interpolation was required. The bilinear interpolation determines the value of the new cell by the weighted distance average of the four nearest input cells. The considered resolution is 25 meters. The maps presented in Appendix E represent the final raster version of each variable.

Following the approach described in chapter 4.1, the probability of each pixel being a flooded area is determined by the computation of a classification random forest algorithm, considering the historical flooded areas in mainland Portugal, after rasterization, as the dependent variable. The independent variables are the ones described in Table II, each one following the same rasterization as the dependent variable. The estimation of the probability is automatically done by the R tool used. According to the good practices in machine learning (Hastie et al (2009)), out of the original data, a training set of 70% of the observations is selected and the tree is grown. The remaining 30% are used as test set and the prediction error is estimated according to the Brier score. The score obtained was of 1.52%, which is relatively small suggesting a proper fit of the probability function to the data and, consequently, of the classification forest.

The importance of each variable according to the Gini importance is presented in Figure 5. Similar to the approaches presented in chapter 4.1, the low elevation and low slope areas are more prone to floods.

---

[2] Process of converting an image described in a vector graphics format (shapes) and converting it into a raster image (series of pixels with the same resolution) (Worboys and Duckham (2004))
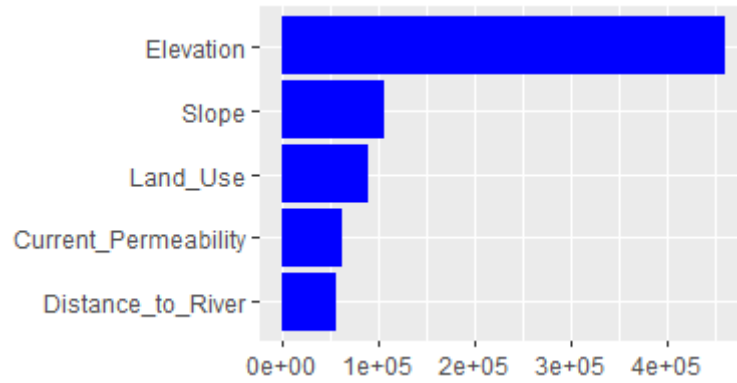
Figure 5 – Importance of each independent variable by Gini importance

Given the high accuracy of the model, the predictions for the probability for original data were mapped for mainland Portugal in Figure 6. In the interest of simplicity, the probabilities were classified into 5 categories by Jenks natural breaks optimization: Very Low, Low, Medium, High and Very High.
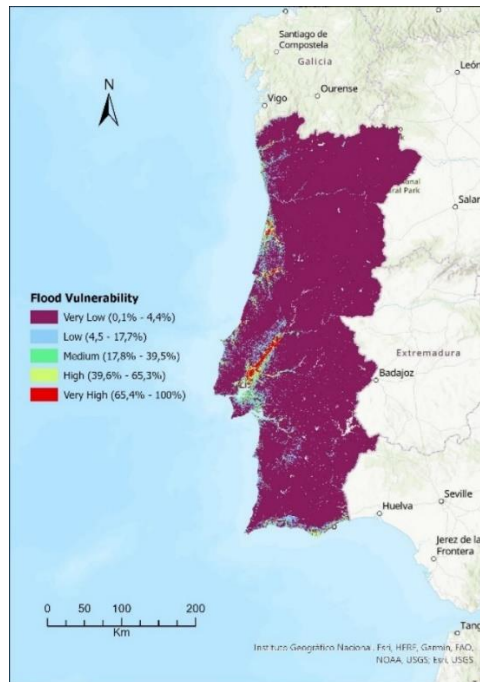
Figure 6 – Flood vulnerability map

5 Climate Change Impact on the Liabilities

The European Union Flood Directive defines flood risk as the convolution of the probability of flood event and the potential harmful consequences to the environment, economy and human beings and states. The Directive also states that the Member States must be coordinated to prevent, protect, and mitigate such effects by the development of effective tools for hazard and flood mapping. A solidary fund for quick financial aid and management plans is suggested (European Parliament (2019)).

Several approaches are available for the calculation of flood risk which combine the concepts defined before. Cançado et al. (2008) consider the risk as a product of hazard and vulnerability where indexes are calculated for both according to the natural, economic, and social variables. Kron (2005) includes the value of humans, items and buildings which considers that, along with hazard and vulnerability, are increasing demanding for the intervention of the people affected, public authorities and insurance companies for risk reduction. Other approaches consider the interaction between hazard, either through classification or just the assessment of the probability of occurrence, and its consequences usually measured in loss of lives and/or the monetary value of structures and items (Meyer et al. (2013)). The hazard mapping is respected as being the most important factor and the other terms are usually included in a broader class which can be identified as the consequences (Klijn et al. (2015)).

In this study, the calculation of the risk is managed by the Equation 4 (Kron (2005)):

$$Risk = Probability\ of\ Occurence \times Vulnerability \times Value \qquad (4)$$

The value of endangered buildings, items and people is given by the sum insured of the insurance company considered in this study. The sum insured is the total of benefits that the insurance company agrees to pay to its policyholder in the event of a natural disaster or other cause that results in major damage, here secured by property insurance contracts. The contracts are grouped in geographical areas to facilitate the calculation of the capital requirements demanded by the Solvency II directive. For Portugal, the division is done by the first two digits of the zip code, which is constituted by 7 digits in the form

XXXX-XXX. The first four digits identify the parish and, the last three identify the street and the building location. This basis was set prior to the parish administrative reorganization (Reorganização Administrativa do Território das Freguesias – Diário da República (2013)), occurred in 2012, therefore current parishes may present two or more 4-digit different combinations. Considering the data for the addresses available at the Portuguese post office service (CTT portal) and the Official Administrative Charter of Portugal from 2011, the following map in Figure 7 was obtained:

Figure 7 - 2-Digit Zip Code Division

For the purpose of addressing the probability of occurrence for different areas under the 2-digit postcode division, the average of the estimated return period variations is calculated for the all the grid points in each area and considering the 100-year historical data thresholds. The use of the 100-year historical data thresholds is used in a number of studies to determine the variation of hydrological variables (Anandalekshmi et al. (2018)) and includes the other two historical thresholds calculated in section 3.3. Then, the probability of incidence of precipitation and river discharge is given by the inverse of the return period, as introduced in section 3.1. A decrease in return period implies an increase in the flood occurrence likelihood because lower return periods correspond to a short

average time between realizations. The probabilities of occurrence for each scenario and climate period are presented in Appendix F.

For all climate scenarios, the average expected increase in the probability of flood occurrence is around one percent, which implies a doubling of the probability of fluvial flood occurrence, given that a return period of 100 years was considered. For the RCP 2.6 scenario, the most probable outcome given the current level of human activity and land system dynamics, the river overflow is projected to rise until mid-century, but then decline. The RCP scenarios 4.5 and 8.5 exhibit lower values for the chance of flooding, which can be explained by the higher global temperatures that are expected to be observed. Although, the evaporation enhancement may lead to higher precipitation levels, the high temperatures lead to prolonged dry periods, decreasing the river discharge values to a state where precipitation will only cover the water shortage enforced in those periods.

The geographical areas where the main Portuguese rivers flow are those where this natural disaster is most frequently anticipated to occur. For instance, in the short-term for the RCP 2.6 scenario, the highest probabilities of overflowing correspond to the rivers Douro, Mondego, Vouga and Lima, located in the northern part of the country, where precipitation levels are higher. Other large rivers with a history of flooding seem to be safer in the next 100 years, such as the Tejo and the Guadiana. For the other climate scenarios, the northern rivers' regions remain those where floods will be prevalent, but with decreased probability. Furthermore, the geographic areas affected by floods appear to change for the different climate developments. For example, in the long term, the RCP 8.5 projections indicate that the Lisbon metropolitan region (areas 11, 12, 13, 14 and 19) will be among those where flooding will occur. However, in the remaining two scenarios,

the forecasts for this region even consider a decrease in these events. This behaviour can be observed in Figure 8:
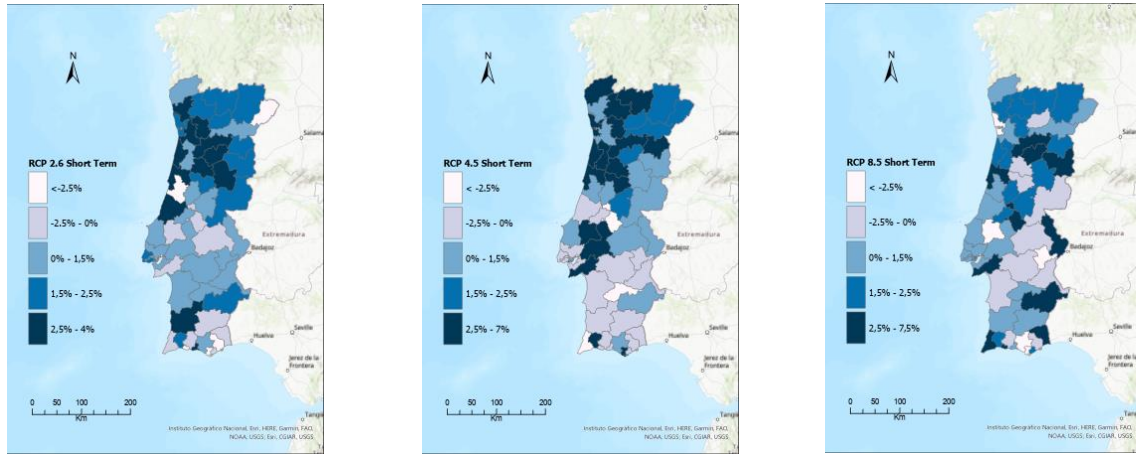
Figure 8 - Probability of occurrence under the RCP 2.6, 4.5 and 8.5 short term scenarios for the different geographical areas

Analogously, the vulnerability to flooding is given by the average of the raster cells in each geographic area. As a result of applying the random forest algorithm to the explanatory variables, as described in section 4.2, regions with low elevation and slopes are more prone to fluvial flooding. A particular landscape where these two characteristics are observed is found in a river estuary. In mainland Portugal, the main rivers originate in mountainous areas located in the interior of the country (where overflow is not possible due to high slopes) and flow on the Atlantic coast. From Figure 9, the Aveiro, Coimbra,

Porto and Santarem areas are those where river floods are most likely to occur, supporting what was observed for the climate scenarios.
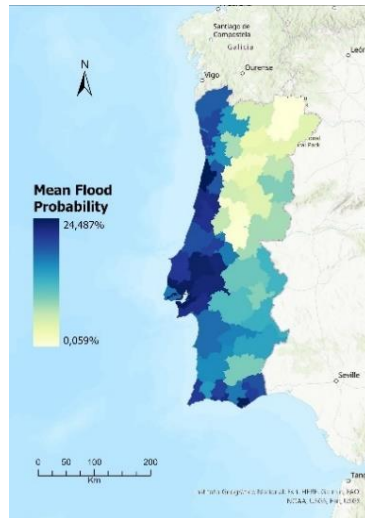
Figure 9 – Mean Flood Probability for the different geographical areas

Following the approach suggested by UNESCO, the flood risk for each geographic area is the product of these estimated probabilities with the value of the properties in the insurer's portfolio. This risk measure allows the insurer to present in its ORSA report, the impact of river flooding on its portfolio, pointing out the areas where losses are expected to be the highest, in addition to the consideration of different climate scenarios that may be experienced until the end of the century. In the specific case of this property insurance portfolio, the insured capital is concentrated in the regions of Aveiro, Coimbra, Lisbon and Porto. The distribution of the insured capital across mainland Portugal is presented in Figure 10:
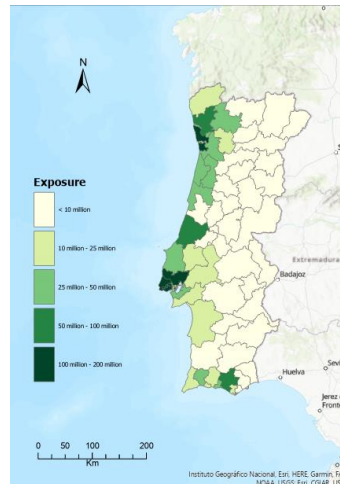
Figure 10 – Exposed insured capital for the different geographical areas

From the findings presented above, these are the areas where fluvial flooding is most likely to occur, and the geographic characteristics render them most vulnerable. Details of the risk for each 2-digit zip code region are presented in Appendix F.

The summary of the flood risk to which the property insurance portfolio is exposed in its full extent is resumed in Table III:

Table III – Risk exposure under the three climate scenarios

| | Probability of Occurrence | | | Vulnerability | Value | Risk | | |
	Short Term	Mid Term	Long Term			Short Term	Mid Term	Long Term
RCP 2.6	0,88%	1,23%	1,03%	4,92%	1 637 207 813,35	712 293,81	991 887,47	829 270,16
RCP 4.5	1,15%	0,75%	0,51%			925 876,79	600 377,07	410 679,29
RCP 8.5	0,68%	0,92%	0,22%			544 609,04	742 325,67	175 369,39

Regardless of the climate scenario, the impact of river floods on the portfolio is small when compared to the total amount insured. However, given the uncertain behaviour of natural catastrophes like floods, the estimates provided may understate the real impact of these phenomena. Climate change plays a key role in the frequency and severity of natural catastrophes, and the losses for insurers are greater than ever before (CRED (2022)). This approach establishes a first basis for an insurance company to assess how significant these risks might be to its business.

6 CONCLUSION

The river flooding phenomenon in Portugal is particularly rare but the increasing pressure of the regulators to address the effects of climate change in the insurers' business demands the analysis of all possible disasters adjacent to extreme weather events. In this study, the risk was assessed by relating two concepts: expected probability of occurrence of the phenomena under the possible climate scenarios and the vulnerability of different regions in mainland Portugal to such events. Based on historical and future data, the variables precipitation and river discharge were considered first individually and then correlated by the usage of copulas. The Gumbel copula due to its upper tail dependency is the one that best describes this interaction. The calculation of the variation of the return period based on historical data are particularly valuable to understand the likelihood of such flood prone conditions ever happening in the future. The RCP 2.6 scenario, the closest scenario to what is being experienced today, suggests an increase in flooding specially for longer terms which may help the insurers to adapt their portfolios. If the other scenarios prove to be the trajectory of the Earths systems, the frequency is expected to decrease.

The application of the random forest classification algorithm to the physical characteristics of the Portuguese territory can serve as a basis for the construction of a flood vulnerability map. Areas with low elevation and slope seem to be the most vulnerable. District capitals such as Aveiro, Coimbra and Oporto, due to their location on the margin of three of the main Portuguese rivers, concentrate valuable goods and items.

The results obtained allow for the determination of the risk level to which the insurer may be exposed in the future. For this insurer, the insured capitals are mainly concentrated in Lisbon and Oporto, one less susceptible than the other.

This approach can be further extended to other weather-related disasters if the data considered is not sparse and the correct variables are considered.

REFERENCES

[1] Abdulkareem, J. H., Pradhan, B., Sulaiman, W. N. A., & Jamil, N. R. (2018). Review of studies on hydrological modelling in Malaysia. *Modeling Earth Systems and Environment*, *4*(4), 1577–1605. https://doi.org/10.1007/s40808-018-0509-y

[2] Adger, W. N. (2006). Vulnerability. *Global Environmental Change*, *16*(3), 268–281. https://doi.org/10.1016/j.gloenvcha.2006.02.006

[3] Anandalekshmi, A., Panicker, S. T., Adarsh, S., Muhammed Siddik, A., Aloysius, S., & Mehjabin, M. (2019). Modeling the concurrent impact of extreme rainfall and reservoir storage on Kerala floods 2018: a Copula approach. *Modeling Earth Systems and Environment*, *5*(4), 1283–1296. https://doi.org/10.1007/s40808-019-00635-6

[4] Barroca, B., Bernardara, P., Mouchel, J. M., & Hubert, G. (2006). Indicators for identification of urban flooding vulnerability. *Natural Hazards and Earth System Sciences*, *6*(4), 553–561. https://doi.org/10.5194/nhess-6-553-2006

[5] Baskot, B., & Stanic, S. (2020). Parametric crop insurance against floods: The case of Bosnia and Herzegovina. *Economic Annals*, *65*(224), 83–100. https://doi.org/10.2298/EKA2024083B

[6] Berg, P, Photiadou, C, Bartosova, A, Biermann, J, Capell, R, Chinyoka, S, Fahlesson, T, Franssen, W, Hundecha, Y, Isberg, K, Ludwig, F, Mook, R, Muzuusa, J, Nauta, L, Rosberg, J, Simonsson, L, Sjökvist, E, Thuresson, J, and van der Linden, E. (2021a): Hydrology related climate impact indicators from 1970 to 2100 derived from bias adjusted European climate projections, version 1, (for 1971-2100, Portugal, E-HYPEgrid, Historical/RCP2.6/RCP4.5/RCP8.5, r1i1p1) . Copernicus Climate Change Service (C3S) Climate Data Store (CDS), (Accessed on 11-JUN-2022), DOI: 10.24381/cds.73237ad6

[7] Berg, P, Photiadou, C, Simonsson, L, Sjökvist, E, Thuresson, J, and Mook, R, (2021b): Temperature and precipitation climate impact indicators from 1970 to 2100 derived from European climate projections, version 1, (for 1971-2100, Portugal, Precipitation, Historical/RCP2.6/RCP4.5/RCP8.5, r1i1p1). Copernicus Climate Change Service (C3S) Climate Data Store (CDS), (Accessed on 11-JUN-2022), DOI: 10.24381/cds.9eed87d5

[8] Blaikie, P., Cannon, T., Davis, I. & Wisner, B., (2005). *At Risk: Natural hazards, people's vulnerability and disasters* (2nd ed.). Taylor & Francis. https://doi.org/10.4324/9780203428764

[9] Breiman, L. (2001). Random Forests. *Machine Learning*, *45*(1), 5–32. https://doi.org/10.1023/A:1010933404324

[10] Cançado, V., Brasil, L., Nascimento, N., & Guerra, A. (2008, August). Flood risk assessment in an urban area: Measuring hazard and vulnerability. *11th International Conference on Urban Drainage*.

[11] Carvalho, A., Schmidt, L., Santos, F. D., & Delicado, A. (2014). Climate change research and policy in Portugal. *WIREs Climate Change*, *5*(2), 199–217. https://doi.org/10.1002/wcc.258

[12] Chan, S. W., Abid, S. K., Sulaiman, N., Nazir, U., & Azam, K. (2022). A systematic review of the flood vulnerability using geographic information system. *Heliyon*, *8*(3), e09075. https://doi.org/10.1016/j.heliyon.2022.e09075

[13] Chowdhary, H., Escobar, L. A., & Singh, V. P. (2011). Identification of suitable copulas for bivariate frequency analysis of flood peak and flood volume data. *Hydrology Research*, *42*(2–3), 193–216. https://doi.org/10.2166/nh.2011.065

[14] Correia, F. N. (1987). Multivariate Partial Duration Series in Flood Risk Analysis. In *Hydrologic Frequency Modeling* (pp. 541–554). Springer Netherlands. https://doi.org/10.1007/978-94-009-3953-0_38

[15] CRED. (2022). *2021 Disasters in numbers*. Date accessed 09/09/2022

[16] Boruff, B. J., Cutter, S. L., & Shirley, W. L. (2012). Social Vulnerability to Environmental Hazards. In *Hazards Vulnerability and Environmental Justice* (1st ed., pp. 243–261). Routledge. https://doi.org/10.4324/9781849771542

[17] ECO Seguros. (2021). Catástrofes naturais: Em Portugal só 9% dos prejuízos estavam seguros. *ECO Seguros*. https://eco.sapo.pt/2021/09/23/catastrofes-naturais-em-portugal-so-9-dos-prejuizos-estavam-seguros/. Date accessed 09/09/2022.

[18] EIOPA. (2019). *Consultation Paper on the Opinion on the 2020 review of Solvency II*. Frankfurt: EIOPA.

[19] EIOPA. (2021). *Opinion on the supervision of the use of climate change risk scenarios in ORSA*. Frankfurt: EIOPA.

[20] EIOPA. (2022). *Application guidance on running climate change materiality assessment and using climate change scenarios in the ORSA*. Frankfurt: EIOPA.

[21] El-Haddad, B. A., Youssef, A. M., Pourghasemi, H. R., Pradhan, B., El-Shater, A.-H., & El-Khashab, M. H. (2021). Flood susceptibility prediction using four machine learning techniques and comparison of their performance at Wadi Qena Basin, Egypt. *Natural Hazards*, *105*(1), 83–114. https://doi.org/10.1007/s11069-020-04296-y

[22] European Parliament. (2009). Directive 2009/138/EC of the European Parliament and of the Council of 25 November 2009 on the taking-up and pursuit of the business of Insurance and Reinsurance (Solvency II). *Official Journal L 335*, 1-155. Retrieved from European Comission: https://ec.europa.eu/info/business-economy-euro/banking-and-finance/insurance-and-pensions/risk-management-and-supervision-insurance-companies-solvency-2_en

[23] European Parliament. (2019). Commission Delegated Regulation (EU) 2019/981 of 8 March 2019 amending Delegated Regulation (EU) 2015/35 supplementing Directive 2009/138/EC of the European Parliament and of the Council on the taking-up and pursuit of the business of Insurance and Reinsurance. *Official Journal L 161*, 1-12.

[24] Falah, F., Rahmati, O., Rostami, M., Ahmadisharaf, E., Daliakopoulos, I. N., & Pourghasemi, H. R. (2019). Artificial Neural Networks for Flood Susceptibility Mapping in Data-Scarce Urban Areas. In *Spatial Modeling in GIS and R for Earth and Environmental Sciences* (pp. 323–336). Elsevier. https://doi.org/10.1016/B978-0-12-815226-3.00014-4

[25] Fatemi, Md. N., Okyere, S. A., Diko, S. K., Kita, M., Shimoda, M., & Matsubara, S. (2020). Physical Vulnerability and Local Responses to Flood Damage in Peri-Urban Areas of Dhaka, Bangladesh. *Sustainability*, *12*(10), 3957. https://doi.org/10.3390/su12103957

[26] Franzke, C. L. E. (2017). Impacts of a Changing Climate on Economic Damages and Insurance. *Economics of Disasters and Climate Change*, *1*(1), 95–110. https://doi.org/10.1007/s41885-017-0004-3

[27] Gumbel, E. J. (1941). The Return Period of Flood Flows. *The Annals of Mathematical Statistics*, *12*(2), 163–190.

[28]   Hastie, T., Tibshirani, R., & Friedman, J. (2009). Random Forests. In *The Elements of Statistical Learning* (2nd ed., pp. 587–602). Springer. https://doi.org/10.1007/b94608_1

[29]   IPCC, 2022: Summary for Policymakers [H.-O. Pörtner, D.C. Roberts, E.S. Poloczanska, K. Mintenbeck, M. Tignor, A. Alegría, M. Craig, S. Langsdorf, S. Löschke, V. Möller, A. Okem (eds.)]. In: Climate Change 2022: Impacts, Adaptation and Vulnerability. Contribution of Working Group II to the Sixth Assessment Report of the Intergovernmental Panel on Climate Change [H.-O. Pörtner, D.C. Roberts, M. Tignor, E.S. Poloczanska, K. Mintenbeck, A. Alegría, M. Craig, S. Langsdorf, S. Löschke, V. Möller, A. Okem, B. Rama (eds.)]. Cambridge University Press, Cambridge, UK and New York, NY, USA, pp. 3–33, doi:10.1017/97810093258

[30]   Jacinto, R., Grosso, N., Reis, E., Dias, L., Santos, F. D., & Garrett, P. (2015). Continental Portuguese Territory Flood Susceptibility Index – contribution to a vulnerability index. *Natural Hazards and Earth System Sciences*, *15*(8), 1907–1919. https://doi.org/10.5194/nhess-15-1907-2015

[31]   Karmakar, S., & Simonovic, S. P. (2009). Bivariate flood frequency analysis. Part 2: a copula-based approach with mixed marginal distributions. *Journal of Flood Risk Management*, *2*(1), 32–44. https://doi.org/10.1111/j.1753-318X.2009.01020.x

[32]   Kazakis, N., Kougias, I., & Patsialis, T. (2015). Assessment of flood hazard areas at a regional scale using an index-based approach and Analytical Hierarchy Process: Application in Rhodope–Evros region, Greece. *Science of The Total Environment*, *538*, 555–563. https://doi.org/10.1016/j.scitotenv.2015.08.055

[33]   Khosravi, K., Nohani, E., Maroufinia, E., & Pourghasemi, H. R. (2016). A GIS-based flood susceptibility assessment and its mapping in Iran: a comparison between frequency ratio and weights-of-evidence bivariate statistical models with multi-criteria decision-making technique. *Natural Hazards*, *83*(2), 947–987. https://doi.org/10.1007/s11069-016-2357-2

[34]   Khosravi, K., Panahi, M., & Tien Bui, D. (2018). Spatial prediction of groundwater spring potential mapping based on an adaptive neuro-fuzzy inference system and metaheuristic optimization. *Hydrology and Earth System Sciences*, *22*(9), 4771–4792. https://doi.org/10.5194/hess-22-4771-2018

[35] Klijn, F., Kreibich, H., de Moel, H., & Penning-Rowsell, E. (2015). Adaptive flood risk management planning based on a comprehensive flood risk conceptualisation. *Mitigation and Adaptation Strategies for Global Change*, *20*(6), 845–864. https://doi.org/10.1007/s11027-015-9638-z

[36] Klein, B., Pahlow, M., Hundecha, Y., & Schumann, A. (2010). Probability Analysis of Hydrological Loads for the Design of Flood Control Systems Using Copulas. *Journal of Hydrologic Engineering*, *15*(5), 360–369. https://doi.org/10.1061/(ASCE)HE.1943-5584.0000204

[37] Kron, W. (2005). Flood Risk = Hazard • Values • Vulnerability. *Water International*, *30*(1), 58–68. https://doi.org/10.1080/02508060508691837

[38] Ko, V., Hjort, N. L., & Hobæk Haff, I. (2019). Focused information criteria for copulas. *Scandinavian Journal of Statistics*, *46*(4), 1117–1140. https://doi.org/10.1111/sjos.12387

[39] Laudan, J., Rözer, V., Sieg, T., Vogel, K., & Thieken, A. H. (2017). Damage assessment in Braunsbach 2016: data collection and analysis for an improved understanding of damaging processes during flash floods. *Natural Hazards and Earth System Sciences*, *17*(12), 2163–2179. https://doi.org/10.5194/nhess-17-2163-2017

[40] Leal, M., Hudson, P., Mobini, S., Sörensen, J., Madeira, P. M., Tesselaar, M., & Zêzere, J. L. (2022). Natural hazard insurance outcomes at national, regional and local scales: A comparison between Sweden and Portugal. *Journal of Environmental Management*, *322*, 116079. https://doi.org/10.1016/j.jenvman.2022.116079

[41] Lee, G., Jun, K.-S., & Chung, E.-S. (2013). Integrated multi-criteria flood vulnerability approach using fuzzy TOPSIS and Delphi technique. *Natural Hazards and Earth System Sciences*, *13*(5), 1293–1312. https://doi.org/10.5194/nhess-13-1293-2013

[42] Lee, S., Kim, J.-C., Jung, H.-S., Lee, M. J., & Lee, S. (2017). Spatial prediction of flood susceptibility using random-forest and boosted-tree models in Seoul metropolitan city, Korea. *Geomatics, Natural Hazards and Risk*, *8*(2), 1185–1203. https://doi.org/10.1080/19475705.2017.1308971

[43] LEAF - Green and Blue Infrastructures. (2022). *EPIC WebGIS Portugal Data*. http://epic-webgis-portugal.isa.ulisboa.pt/data

[44]   Madsen, H., Lawrence, D., Lang, M., Martinkova, M., & Kjeldsen, T. R. (2014). Review of trend analysis and climate change projections of extreme precipitation and floods in Europe. *Journal of Hydrology*, *519*, 3634–3650. https://doi.org/10.1016/j.jhydrol.2014.11.003

[45]   Malekian, A., & Azarnivand, A. (2016). Application of Integrated Shannon's Entropy and VIKOR Techniques in Prioritization of Flood Risk in the Shemshak Watershed, Iran. *Water Resources Management*, *30*(1), 409–425. https://doi.org/10.1007/s11269-015-1169-6

[46]   Malley, J. D., Kruppa, J., Dasgupta, A., Malley, K. G., & Ziegler, A. (2012). Probability Machines. *Methods of Information in Medicine*, *51*(01), 74–81. https://doi.org/10.3414/ME00-01-0052

[47]   Messner, F., & Meyer, V. (2006). Flood Damage, Vulnerability and Risk Perception – Challenges for Flood Damage Research. In *Flood Risk Management: Hazards, Vulnerability and Mitigation Measures* (pp. 149–167). Springer Netherlands. https://doi.org/10.1007/978-1-4020-4598-1_13

[48]   Meyer, V., Becker, N., Markantonis, V., Schwarze, R., van den Bergh, J. C. J. M., Bouwer, L. M., Bubeck, P., Ciavola, P., Genovese, E., Green, C., Hallegatte, S., Kreibich, H., Lequeux, Q., Logar, I., Papyrakis, E., Pfurtscheller, C., Poussin, J., Przyluski, V., Thieken, A. H., & Viavattene, C. (2013). Review article: Assessing the costs of natural hazards – state of the art and knowledge gaps. *Natural Hazards and Earth System Sciences*, *13*(5), 1351–1373. https://doi.org/10.5194/nhess-13-1351-2013

[49]   Nelsen, R. B. (n.d.). Archimedean Copulas. In *An Introduction to Copulas* (pp. 109–155). Springer New York. https://doi.org/10.1007/0-387-28678-0_4

[50]   Olowe, F. J. (2021). *Spatial Prediction of Flood Susceptible Areas Using Machine Learning Approach: A Focus on West African Region*.

[51]   Prettenthaler, F., Albrecher, H., Asadi, P., & Köberl, J. (2017). On flood risk pooling in Europe. *Natural Hazards*, *88*(1), 1–20. https://doi.org/10.1007/s11069-016-2616-2

[52]   Prudential Regulation Authority. (2016). *Supervisory Statement - SS19/16 Solvency II: ORSA*. London: Bank of England.

[53]   Rehman, S., Sahana, M., Hong, H., Sajjad, H., & Ahmed, B. bin. (2019). A systematic review on approaches and methods used for flood vulnerability assessment: framework for future research. *Natural Hazards*, *96*(2), 975–998. https://doi.org/10.1007/s11069-018-03567-z

[54]   Saf, B. (2009). Regional Flood Frequency Analysis Using L-Moments for the West Mediterranean Region of Turkey. *Water Resources Management*, *23*(3), 531–551. https://doi.org/10.1007/s11269-008-9287-z

[55]   Salvadori, G., & De Michele, C. (2004). Frequency analysis via copulas: Theoretical aspects and applications to hydrological events. *Water Resources Research*, *40*(12). https://doi.org/10.1029/2004WR003133

[56]   Samanta, S., Pal, D. K., & Palsamanta, B. (2018). Flood susceptibility analysis through remote sensing, GIS and frequency ratio model. *Applied Water Science*, *8*(2), 66. https://doi.org/10.1007/s13201-018-0710-1

[57]   Seneviratne, S.I., X. Zhang, M. Adnan, W. Badi, C. Dereczynski, A. Di Luca, S. Ghosh, I. Iskandar, J. Kossin, S. Lewis, F. Otto, I. Pinto, M. Satoh, S.M. Vicente-Serrano, M. Wehner, and B. Zhou, 2021: Weather and Climate Extreme Events in a Changing Climate. In Climate Change 2021: The Physical Science Basis. Contribution of Working Group I to the Sixth Assessment Report of the Intergovernmental Panel on Climate Change [Masson-Delmotte, V., P. Zhai, A. Pirani, S.L. Connors, C. Péan, S. Berger, N. Caud, Y. Chen, L. Goldfarb, M.I. Gomis, M. Huang, K. Leitzell, E. Lonnoy, J.B.R. Matthews, T.K. Maycock, T. Waterfield, O. Yelekçi, R. Yu, and B. Zhou (eds.)]. Cambridge University Press, Cambridge, United Kingdom and New York, NY, USA, pp. 1513–1766, doi:10.1017/9781009157896.013

[58]   Shafapour Tehrany, M., Kumar, L., Neamah Jebur, M., & Shabani, F. (2019). Evaluating the application of the statistical index method in flood susceptibility mapping and its comparison with frequency ratio and logistic regression methods. *Geomatics, Natural Hazards and Risk*, *10*(1), 79–101. https://doi.org/10.1080/19475705.2018.1506509

[59]   Shafizadeh-Moghadam, H., Valavi, R., Shahabi, H., Chapi, K., & Shirzadi, A. (2018). Novel forecasting approaches using combination of machine learning and

statistical models for flood susceptibility mapping. *Journal of Environmental Management*, *217*, 1–11. https://doi.org/10.1016/j.jenvman.2018.03.089

[60]   Siahkamari, S., Haghizadeh, A., Zeinivand, H., Tahmasebipour, N., & Rahmati, O. (2018). Spatial prediction of flood-susceptible areas using frequency ratio and maximum entropy models. *Geocarto International*, *33*(9), 927–941. https://doi.org/10.1080/10106049.2017.1316780

[61]   Tehrany, M. S., Pradhan, B., & Jebur, M. N. (2014). Flood susceptibility mapping using a novel ensemble weights-of-evidence and support vector machine models in GIS. *Journal of Hydrology*, *512*, 332–343. https://doi.org/10.1016/j.jhydrol.2014.03.008

[62]   Turner, G., Said, F., & Afzal, U. (2014). Microinsurance Demand After a Rare Flood Event: Evidence From a Field Experiment in Pakistan. *The Geneva Papers on Risk and Insurance - Issues and Practice*, *39*(2), 201–223. https://doi.org/10.1057/gpp.2014.8

[63]   van Vuuren, D. P., Edmonds, J., Kainuma, M., Riahi, K., Thomson, A., Hibbard, K., Hurtt, G. C., Kram, T., Krey, V., Lamarque, J.-F., Masui, T., Meinshausen, M., Nakicenovic, N., Smith, S. J., & Rose, S. K. (2011). The representative concentration pathways: an overview. *Climatic Change*, *109*(1–2), 5–31. https://doi.org/10.1007/s10584-011-0148-z

[64]   Vojtek, M., & Vojteková, J. (2019). Flood Susceptibility Mapping on a National Scale in Slovakia Using the Analytical Hierarchy Process. *Water*, *11*(2), 364. https://doi.org/10.3390/w11020364

[65]   Wen, T., Jiang, C., & Xu, X. (2019). Nonstationary Analysis for Bivariate Distribution of Flood Variables in the Ganjiang River Using Time-Varying Copula. *Water*, *11*(4), 746. https://doi.org/10.3390/w11040746

[66]   Worboys, M. F., & Duckham, M. (2004). *GIS: A Computing Perspective*. CRC Press. https://doi.org/10.4324/9780203481554

[67]   Yin, J., Guo, S., He, S., Guo, J., Hong, X., & Liu, Z. (2018). A copula-based analysis of projected climate changes to bivariate flood quantiles. *Journal of Hydrology*, *566*, 23–42. https://doi.org/10.1016/j.jhydrol.2018.08.053

[68]   Yue, S. (2001). A Bivariate Extreme Value Distribution Applied to Flood Frequency Analysis. *Hydrology Research*, *32*(1), 49–64. https://doi.org/10.2166/nh.2001.0004

[69]   Zêzere, J. L., Pereira, A. R., & Morgado, P. (2006). Perigos naturais e tecnológicos no território de Portugal Continental. *Apontamentos de Geografia-Série Investigação*, *19*.

[70]   Zhang, L., & Singh, V. P. (2007). Trivariate Flood Frequency Analysis Using the Gumbel–Hougaard Copula. *Journal of Hydrologic Engineering*, *12*(4), 431–439. https://doi.org/10.1061/(ASCE)1084-0699(2007)12:4(431)

A - Representative Concentration Pathways

Scenario	Radiative Forcing	Concentration	Pathway
RCP 2.6	Peak in radiative forcing[1] at ~3 W/m² before 2100 and then decline (the selected pathway declines to 2.6 W/m² by 2100)	peak at ~490 ppm CO2 eq before 2100 and then decline	Peak and decline
RCP 4.5	~4.5 W/m² at stabilization after 2100	~650 ppm CO2 eq at stabilization after 2100	Stabilization without overshoot
RCP 6	~6 W/m² at stabilization after 2100	~850 ppm CO2 eq at stabilization after 2100	Stabilization without overshoot
RCP 8.5	>8.5 W/m² by 2100	> ~1370 ppm CO2 eq by 2100	Rising

[1] Change on the amount of downward-directed radiant energy impinging upon Earth's surface due to anthropogenic climate change factors. Is measured in watts per square metre (W/m2).

B - Archimedean Copulas Generator Functions

Copula	Generator $\varphi(t)$
Ali-Mikhail-Haq	$\varphi(t) = \dfrac{1 - \theta}{\exp(t) - \theta} , \theta \in [0,1[$
Clayton	$\varphi(t) = (1 + t)^{-\frac{1}{\theta}} , \theta \in [0, \infty[$
Frank	$\varphi(t) = -\dfrac{\log(1 - (1 - \exp(-\theta))\exp(-t))}{\theta}$ $\theta \in]0, \infty[$

Gumbel	$\varphi(t) = \exp(-t^{\frac{1}{\theta}}), \theta \in [1, \infty[$
Joe	$\varphi(t) = 1 - (1 - \exp(-t))^{\frac{1}{\theta}}, \theta \in [1, \infty[$

C – Margins' Density Functions

Distribution	Probability Density Function
Exponential	$$f(x) = \frac{1}{scale} * \exp\left(-\frac{x - loc}{scale}\right)$$ $$rate = \frac{1}{scale}$$
Gamma	$$f(x) = \frac{\left(\frac{x - loc}{scale}\right)^{\alpha - 1} \exp -\left(\frac{x - loc}{scale}\right)}{scale * \Gamma(\alpha)}$$ $$\alpha = shape, \beta = \frac{1}{scale}$$
Generalized Logistic	$$f(x) = c\frac{1}{scale}\frac{\exp\left(-\frac{x - loc}{scale}\right)}{\left(1 + \exp\left(-\frac{x - loc}{scale}\right)\right)^{c+1}}$$
Generalized Pareto	$$f(x) = \frac{1}{scale} * \left(1 + c\left(\frac{x - loc}{scale}\right)\right)^{-1-\frac{1}{c}}$$ $$c = shape$$
Generalized Extreme Value	$$f(x) = \frac{1}{scale}\exp\left[-\left(1 - c\left(\frac{x - loc}{scale}\right)\right)^{1/c}\right] * \left(1 - c\left(\frac{x - loc}{scale}\right)\right)^{\frac{1}{c}-1}$$ $$c = shape$$
Gumbel	$$f(x) = \frac{1}{scale}\exp\left(-\left(\frac{x - loc}{scale} + \exp\left(-\frac{x - loc}{scale}\right)\right)\right)$$
Lognormal	$$f(x) = \frac{1}{s\left(\frac{x - loc}{scale}\right)\sqrt{2\pi}}\exp\left(\frac{\log^2\left(\frac{x - loc}{scale}\right)}{2s^2}\right)$$ $$s = shape$$
Normal	$$f(x) = \frac{\exp\left(-0.5\left(\frac{x - loc}{scale}\right)^2\right)}{scale * \sqrt{2\pi}}$$

Pearson III	$$f(x) = \frac{1}{scale} \frac{|\beta|}{\Gamma(\alpha)} \left[\beta \left(\left(\frac{x - loc}{scale} \right) - \zeta \right) \right]^{\alpha - 1} * \exp\left(-\beta \left(\left(\frac{x - loc}{scale} \right) - \zeta \right) \right)$$ $$\kappa = shape, \beta = \frac{2}{\kappa}, \alpha = \beta^2 = \frac{4}{\kappa^2}, \zeta = -\beta$$
Weibull	$$f(x) = \frac{1}{scale} c \left(\frac{x - loc}{scale} \right)^{c-1} \exp\left(-\left(\frac{x - loc}{scale} \right)^c \right)$$ $$c = shape$$

D – Copernicus Data Details

- *Precipitation* – deposition of water to the Earth's surface in the form of rain, snow, ice or hail:
  - Units: $kg\ m^{-2}\ s^{-1}$
  - Projection: Lambert azimuthal equal area and rotated grid
  - Resolution: 5km x 5km
  - Temporal coverage: Daily data from 1971-2100
  - Climate scenarios: Historical (1971-2005), RCP 2.6 (2005-2100), RCP 4.5 (2005-2100), and RCP 8.5 (2005-2100)

- *River Discharge* – Volume rate of water flow that is transported through a given cross-sectional area:
  - Units: $m^3\ s^{-1}$
  - Projection: Lambert azimuthal equal area and rotated grid
  - Resolution: 5km x 5km
  - Temporal coverage: Daily data from 1971-2100
  - Climate scenarios: Historical (1971-2005), RCP 2.6 (2005-2100), RCP 4.5 (2005-2100), and RCP 8.5 (2005-2100)

E - Spatial datasets for flood vulnerability probability estimation
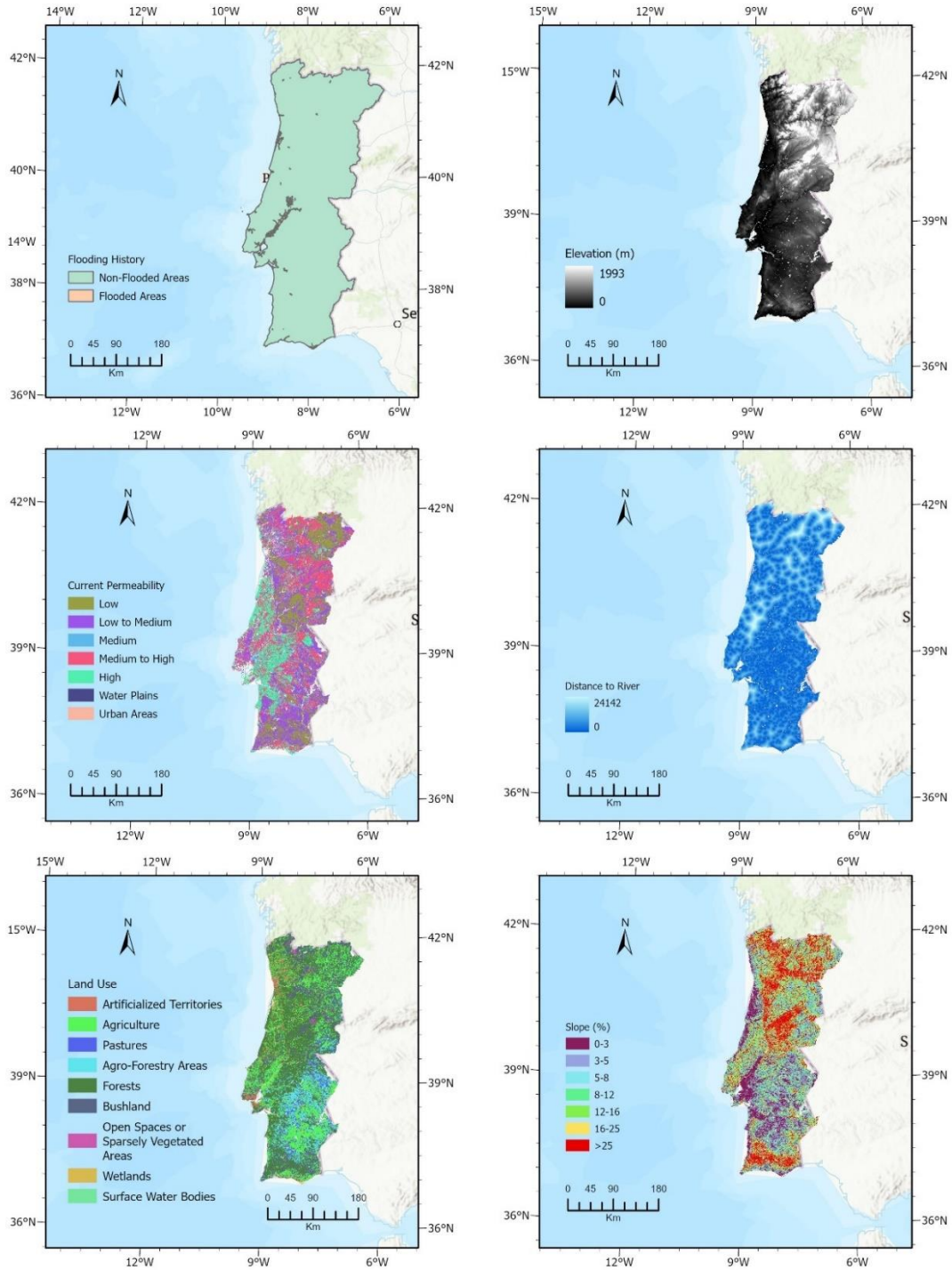
F - Risk Factors under the Climate Scenarios

The highlighted probabilities of occurrence refer to areas not covered by the grid points.
An average of the probability for the surrounding areas was considered.

RCP 2.6

Areas	Probability of Occurrence			Vulnerability	Value	Risk		
	Short Term	MidTerm	Long Term			Short Term	Mid Term	Long Term
10	-0,31%	-0,59%	1,62%	2,97%	113 500 991,05	-10556,76	-20056,61	54685,27
11	1,26%	1,29%	1,27%	13,70%	64 443 223,06	111357,51	113692,79	112287,16
12	1,23%	1,21%	1,34%	8,95%	67 743 672,59	74557,20	73614,15	81507,74
13	1,23%	1,21%	1,34%	8,54%	23 562 602,76	24754,82	24441,70	27062,57
14	1,33%	1,32%	1,37%	8,40%	11 288 421,35	12612,24	12544,05	12967,83
15	1,51%	1,09%	1,35%	1,96%	18 193 985,11	5370,94	3893,93	4788,01
16	-0,57%	-1,10%	1,39%	2,76%	36 582 259,17	-5722,29	-11090,38	14055,33
17	-0,06%	-0,09%	1,85%	2,52%	20 103 197,49	-300,02	-460,38	9367,00
18	1,26%	2,77%	0,62%	21,17%	14 424 274,90	38593,69	84712,60	18909,17
19	1,26%	1,29%	1,27%	24,46%	25 033 741,82	77215,57	78834,86	77860,19
20	-0,03%	0,57%	4,00%	15,30%	11 903 812,21	-612,32	10424,86	72790,70
21	0,71%	-3,99%	3,49%	10,60%	17 553 681,75	13265,39	-74326,41	64990,82
22	-0,16%	-1,16%	0,54%	1,45%	3 039 646,47	-69,48	-510,68	237,85
23	0,83%	-3,79%	2,11%	3,78%	6 305 625,05	1971,27	-9038,51	5033,37
24	3,87%	3,17%	1,30%	3,09%	69 082 702,58	82595,96	67668,21	27830,17
25	1,38%	-2,19%	0,52%	6,21%	30 746 427,34	26341,87	-41863,19	9998,51
26	1,44%	6,80%	-0,72%	16,91%	108 803 304,15	264680,75	1250280,48	-133041,54
27	2,41%	1,62%	0,73%	2,40%	173 928 789,08	100609,25	67471,02	30494,03
28	0,08%	0,46%	2,44%	19,11%	47 351 179,33	6919,33	41660,64	221138,50
29	-0,05%	-0,58%	0,94%	7,83%	21 162 334,99	-753,60	-9591,76	15503,59
30	3,39%	1,50%	1,69%	8,69%	26 043 221,51	76584,47	33916,79	38286,19
31	-3,73%	3,16%	2,03%	6,89%	8 374 801,92	-21542,57	18259,31	11687,06
32	0,86%	3,04%	0,19%	0,26%	5 868 329,21	128,61	454,96	28,96
33	1,96%	-0,02%	0,21%	0,10%	1 236 919,95	24,41	-0,20	2,62
34	3,02%	-1,32%	1,18%	0,23%	8 060 041,32	569,60	-248,83	223,68
35	3,59%	2,12%	0,96%	0,18%	8 745 608,18	565,27	334,23	151,57

36	2,77%	2,90%	1,46%	0,12%	5 250 839,44	174,50	182,33	91,58
37	0,46%	1,56%	-3,78%	3,04%	25 556 734,36	3553,18	12084,02	-29386,34
38	3,12%	1,62%	1,06%	24,49%	27 605 346,78	211163,04	109268,94	71528,70
40	**1,92%**	**2,22%**	**3,09%**	2,43%	40 903 849,20	19030,16	22097,49	30656,88
41	**1,92%**	**2,22%**	**3,09%**	5,94%	30 562 312,78	34745,24	40345,58	55973,30
42	**1,92%**	**2,22%**	**3,09%**	1,68%	9 953 119,19	3206,72	3723,59	5165,91
43	-1,35%	1,84%	3,45%	4,00%	2 384 212,39	-1289,07	1757,93	3287,08
44	1,92%	2,22%	3,09%	6,14%	124 356 525,14	146304,29	169886,03	235690,81
45	3,29%	1,53%	1,82%	0,96%	44 452 951,08	14094,42	6563,10	7772,10
46	3,02%	2,09%	-8,97%	0,29%	14 569 072,39	1269,43	877,16	-3768,72
47	3,43%	1,72%	-0,93%	3,26%	89 040 683,89	99787,91	49927,13	-27147,76
48	2,03%	2,17%	3,77%	0,88%	25 000 041,81	4436,37	4759,00	8254,17
49	0,23%	1,67%	1,33%	2,88%	17 673 224,83	1159,82	8498,37	6761,26
50	1,94%	1,21%	1,01%	0,17%	5 375 072,49	177,06	110,89	92,01
51	1,46%	3,25%	1,02%	0,19%	4 700 199,73	129,13	287,42	90,05
52	-5,10%	1,52%	1,45%	0,19%	1 907 460,69	-189,75	56,38	53,99
53	1,90%	5,72%	0,98%	0,06%	3 985 400,31	44,77	134,88	23,15
54	2,09%	2,17%	0,69%	0,22%	7 447 977,04	340,79	354,01	113,09
60	1,71%	0,71%	0,98%	0,30%	5 019 973,78	255,47	106,16	146,36
61	1,33%	-3,07%	-0,78%	0,08%	2 097 878,81	22,25	-51,37	-13,02
62	3,77%	2,67%	0,54%	0,20%	5 194 922,20	387,16	274,11	55,81
63	1,83%	2,01%	2,14%	0,34%	2 711 768,29	167,88	184,40	196,74
64	1,58%	1,36%	1,93%	0,26%	580 527,01	24,23	20,84	29,45
70	0,61%	6,07%	-3,04%	0,55%	8 937 517,84	303,06	3003,62	-1502,17
71	1,23%	7,15%	0,09%	0,33%	1 829 822,15	74,47	433,00	5,28
72	0,88%	1,77%	3,78%	0,66%	903 045,44	52,76	106,27	226,65
73	1,09%	1,01%	0,91%	0,61%	3 792 942,38	250,44	231,89	210,45
74	-0,99%	0,44%	1,66%	0,45%	2 044 023,78	-90,37	40,49	152,43
75	0,05%	-1,20%	1,34%	2,77%	11 693 922,84	173,67	-3882,46	4329,89
76	3,12%	1,14%	1,66%	1,07%	1 796 719,08	597,51	218,95	318,48
77	-0,40%	0,50%	-1,04%	0,35%	1 103 085,21	-15,29	19,25	-40,29
78	1,80%	0,27%	0,49%	0,78%	5 602 875,18	790,34	119,66	215,59
79	0,52%	-0,12%	-0,29%	1,25%	4 718 964,70	307,82	-71,67	-173,06
80	-4,37%	0,32%	4,01%	19,40%	11 401 536,28	-96724,38	7149,53	88786,86

81	1,02%	-1,20%	3,24%	1,98%	52 129 387,79	10532,41	-12400,05	33484,29
82	2,62%	-0,50%	3,57%	8,19%	25 870 547,09	55513,98	-10606,62	75562,80
83	-0,19%	-0,79%	1,59%	3,72%	12 122 808,10	-862,13	-3582,64	7174,98
84	-2,81%	5,08%	1,53%	7,08%	12 568 098,21	-25053,54	45254,93	13604,02
86	-1,92%	3,43%	-6,85%	4,41%	21 644 520,99	-18334,15	32778,65	-65414,05
87	-1,27%	-0,18%	1,24%	17,00%	6 774 300,91	-14678,07	-2123,41	14320,40
88	-4,93%	-1,92%	-2,76%	4,03%	6 460 750,46	-12849,86	-5012,00	-7181,95
89	-0,74%	1,19%	2,38%	3,06%	6 400 056,95	-1453,59	2340,66	4673,28

RCP 4.5

Areas	Probability of Occurrence			Vulnerability	Value	Risk		
	Short Term	MidTerm	Long Term			Short Term	Mid Term	Long Term
10	-0,38%	-0,33%	0,67%	2,97%	113 500 991,05	-12907,46	-10999,22	22657,70
11	1,40%	1,39%	1,37%	13,70%	64 443 223,06	123489,02	122370,59	121146,25
12	1,26%	1,27%	1,32%	8,95%	67 743 672,59	76578,78	77222,67	79986,45
13	1,26%	1,27%	1,32%	8,54%	23 562 602,76	25426,03	25639,82	26557,47
14	1,55%	1,52%	1,51%	8,40%	11 288 421,35	14748,06	14425,29	14341,44
15	0,20%	2,98%	0,09%	1,96%	18 193 985,11	695,46	10604,03	307,29
16	-0,50%	-0,58%	-0,14%	2,76%	36 582 259,17	-5008,43	-5859,75	-1392,90
17	-0,27%	-0,07%	1,48%	2,52%	20 103 197,49	-1363,34	-363,91	7498,25
18	-1,01%	-0,21%	0,84%	21,17%	14 424 274,90	-30876,15	-6459,89	25682,08
19	1,40%	1,39%	1,37%	24,46%	25 033 741,82	85627,59	84852,07	84003,10
20	6,62%	-0,59%	-0,35%	15,30%	11 903 812,21	120564,78	-10678,02	-6447,43
21	2,80%	-2,89%	2,16%	10,60%	17 553 681,75	52018,15	-53774,74	40160,26
22	-3,60%	-2,34%	1,51%	1,45%	3 039 646,47	-1590,28	-1032,09	664,26
23	-0,56%	-0,63%	3,45%	3,78%	6 305 625,05	-1331,57	-1489,83	8233,09
24	-0,18%	8,25%	-0,92%	3,09%	69 082 702,58	-3857,90	176225,63	-19695,71
25	0,54%	-1,85%	0,27%	6,21%	30 746 427,34	10271,60	-35259,83	5192,21
26	-1,32%	-0,43%	0,41%	16,91%	108 803 304,15	-242630,49	-78286,22	74639,49
27	-1,45%	-0,14%	0,64%	2,40%	173 928 789,08	-60284,93	-5725,30	26556,80
28	-0,49%	-0,93%	0,31%	19,11%	47 351 179,33	-44573,29	-83877,02	28256,01
29	3,27%	-0,86%	0,06%	7,83%	21 162 334,99	54196,20	-14180,03	1068,83
30	4,74%	1,61%	6,02%	8,69%	26 043 221,51	107230,07	36489,25	136120,33
31	0,85%	1,75%	-0,59%	6,89%	8 374 801,92	4881,91	10123,01	-3401,80

32	0,17%	0,81%	1,71%	0,26%	5 868 329,21	25,43	122,07	255,70
33	2,74%	1,48%	-1,68%	0,10%	1 236 919,95	34,08	18,43	-20,91
34	6,10%	6,68%	1,92%	0,23%	8 060 041,32	1151,44	1262,37	362,86
35	1,91%	4,44%	2,23%	0,18%	8 745 608,18	300,12	699,74	350,96
36	3,42%	2,66%	3,24%	0,12%	5 250 839,44	215,00	167,63	203,80
37	4,37%	2,85%	5,32%	3,04%	25 556 734,36	33934,14	22142,64	41299,53
38	5,08%	0,61%	4,01%	24,49%	27 605 346,78	343181,88	41344,55	270878,91
40	2,95%	2,36%	-0,34%	2,43%	40 903 849,20	29311,75	23402,18	-3347,18
41	2,95%	2,36%	-0,34%	5,94%	30 562 312,78	53517,36	42727,67	-6111,28
42	2,95%	2,36%	-0,34%	1,68%	9 953 119,19	4939,24	3943,44	-564,02
43	-0,11%	-0,47%	-0,74%	4,00%	2 384 212,39	-102,88	-448,91	-708,35
44	2,95%	2,36%	-0,34%	6,14%	124 356 525,14	225349,40	179916,50	-25733,21
45	1,43%	-1,01%	1,56%	0,96%	44 452 951,08	6103,72	-4337,52	6697,52
46	3,00%	2,95%	2,07%	0,29%	14 569 072,39	1260,51	1238,13	870,07
47	0,61%	6,58%	-0,49%	3,26%	89 040 683,89	17615,44	191091,29	-14202,82
48	6,39%	0,36%	-7,85%	0,88%	25 000 041,81	13984,14	796,96	-17177,89
49	4,06%	2,80%	0,88%	2,88%	17 673 224,83	20668,71	14281,42	4483,26
50	2,09%	1,24%	3,92%	0,17%	5 375 072,49	190,90	113,70	358,45
51	1,84%	1,32%	1,25%	0,19%	4 700 199,73	162,55	116,85	110,35
52	2,30%	-0,75%	-0,57%	0,19%	1 907 460,69	85,43	-27,94	-21,35
53	2,10%	-0,09%	0,44%	0,06%	3 985 400,31	49,50	-2,01	10,34
54	2,71%	2,24%	2,31%	0,22%	7 447 977,04	441,73	365,72	377,55
60	0,80%	0,07%	0,17%	0,30%	5 019 973,78	119,85	10,10	24,88
61	2,01%	-0,90%	0,12%	0,08%	2 097 878,81	33,67	-15,14	2,05
62	0,86%	1,39%	-2,65%	0,20%	5 194 922,20	88,51	142,49	-272,53
63	0,15%	0,16%	-0,84%	0,34%	2 711 768,29	13,37	14,37	-77,25
64	4,24%	3,14%	4,41%	0,26%	580 527,01	64,77	48,01	67,39
70	-0,58%	-4,18%	0,00%	0,55%	8 937 517,84	-288,56	-2068,52	0,65
71	-1,83%	-0,87%	-0,25%	0,33%	1 829 822,15	-110,76	-52,48	-14,90
72	-0,18%	0,55%	0,03%	0,66%	903 045,44	-10,62	32,80	1,54
73	0,04%	-3,57%	-0,35%	0,61%	3 792 942,38	8,24	-823,38	-80,57
74	0,32%	7,45%	0,29%	0,45%	2 044 023,78	29,01	682,04	26,23
75	-0,19%	0,43%	-0,17%	2,77%	11 693 922,84	-600,22	1389,94	-537,97
76	-0,41%	-1,30%	-0,16%	1,07%	1 796 719,08	-78,22	-248,67	-29,88

77	-0,81%	-0,36%	-0,22%	0,35%	1 103 085,21	-31,30	-13,89	-8,49
78	0,34%	1,10%	0,42%	0,78%	5 602 875,18	150,99	484,00	181,98
79	-3,26%	2,75%	0,33%	1,25%	4 718 964,70	-1929,54	1624,84	196,49
80	3,04%	-0,17%	0,45%	19,40%	11 401 536,28	67245,92	-3842,98	10053,99
81	0,10%	-0,60%	-0,92%	1,98%	52 129 387,79	1014,94	-6160,10	-9492,75
82	-0,41%	-4,95%	-7,13%	8,19%	25 870 547,09	-8656,72	-104881,51	-151146,56
83	-0,16%	-1,68%	-2,25%	3,72%	12 122 808,10	-712,22	-7595,73	-10150,69
84	-0,26%	-0,53%	3,38%	7,08%	12 568 098,21	-2314,89	-4717,10	30056,69
86	-3,06%	-0,26%	-0,20%	4,41%	21 644 520,99	-29270,63	-2445,54	-1869,76
87	-0,28%	-0,13%	-0,33%	17,00%	6 774 300,91	-3275,28	-1518,03	-3766,42
88	-0,23%	-0,33%	-0,28%	4,03%	6 460 750,46	-610,09	-871,68	-720,18
89	-0,10%	-0,23%	-0,13%	3,06%	6 400 056,95	-193,17	-444,81	-260,40

RCP 8.5

Areas	Probability of Occurrence			Vulnerability	Value	Risk		
	Short Term	MidTerm	Long Term			Short Term	Mid Term	Long Term
10	1,51%	0,69%	-1,02%	2,97%	113 500 991,05	50980,98	23397,58	-34448,73
11	1,15%	1,21%	2,01%	13,70%	64 443 223,06	101575,14	106769,86	177870,97
12	1,45%	1,20%	2,08%	8,95%	67 743 672,59	88189,05	72716,36	126069,85
13	1,45%	1,20%	2,08%	8,54%	23 562 602,76	29280,93	24143,62	41858,28
14	1,26%	1,30%	2,18%	8,40%	11 288 421,35	11960,10	12320,96	20669,33
15	1,38%	-1,50%	0,38%	1,96%	18 193 985,11	4924,19	-5321,18	1358,49
16	1,30%	1,39%	-0,70%	2,76%	36 582 259,17	13114,39	14032,93	-7072,36
17	1,72%	0,00%	-1,34%	2,52%	20 103 197,49	8726,91	-11,88	-6793,79
18	1,06%	3,67%	-0,57%	21,17%	14 424 274,90	32474,19	111952,54	-17269,42
19	1,15%	1,21%	2,01%	24,46%	25 033 741,82	70432,45	74034,48	123336,17
20	-6,23%	0,44%	-0,25%	15,30%	11 903 812,21	-113458,59	8104,78	-4566,59
21	0,44%	1,58%	-0,14%	10,60%	17 553 681,75	8253,56	29489,60	-2569,29
22	2,87%	2,26%	-0,04%	1,45%	3 039 646,47	1265,35	999,10	-19,15
23	1,61%	1,48%	-0,23%	3,78%	6 305 625,05	3835,17	3526,88	-542,63
24	1,40%	-7,08%	-0,23%	3,09%	69 082 702,58	29919,21	-151150,26	-4983,34
25	0,50%	4,70%	-0,36%	6,21%	30 746 427,34	9558,89	89817,55	-6810,84
26	0,42%	2,36%	-0,18%	16,91%	108 803 304,15	76777,91	433950,66	-32379,56
27	1,05%	8,64%	-0,18%	2,40%	173 928 789,08	43783,88	360457,63	-7467,53

28	1,21%	4,61%	-0,33%	19,11%	47 351 179,33	109641,93	417444,09	-30064,40
29	5,07%	3,58%	-0,18%	7,83%	21 162 334,99	84070,33	59355,14	-2922,60
30	7,54%	-3,00%	-2,39%	8,69%	26 043 221,51	170662,64	-67767,09	-53985,37
31	1,31%	5,06%	-2,05%	6,89%	8 374 801,92	7585,27	29193,85	-11823,35
32	2,19%	0,17%	-2,27%	0,26%	5 868 329,21	327,61	24,90	-340,77
33	-0,28%	-0,37%	-2,89%	0,10%	1 236 919,95	-3,44	-4,59	-35,96
34	-0,86%	-3,60%	1,60%	0,23%	8 060 041,32	-161,56	-680,77	301,72
35	2,57%	1,76%	1,33%	0,18%	8 745 608,18	404,03	277,27	209,69
36	3,76%	2,00%	1,00%	0,12%	5 250 839,44	236,39	125,84	62,76
37	2,45%	6,56%	1,67%	3,04%	25 556 734,36	19034,45	50986,55	12992,96
38	2,43%	-1,33%	2,15%	24,49%	27 605 346,78	164099,99	-89779,86	145183,55
40	**-6,14%**	**-0,37%**	**1,52%**	2,43%	40 903 849,20	-61005,00	-3678,06	15115,77
41	**-6,14%**	**-0,37%**	**1,52%**	5,94%	30 562 312,78	-111382,87	-6715,40	27598,35
42	**-6,14%**	**-0,37%**	**1,52%**	1,68%	9 953 119,19	-10279,79	-619,78	2547,12
43	-0,13%	-0,79%	-0,78%	4,00%	2 384 212,39	-119,90	-757,82	-746,71
44	-6,14%	-0,37%	1,52%	6,14%	124 356 525,14	-469007,88	-28277,01	116210,37
45	0,46%	0,09%	1,95%	0,96%	44 452 951,08	1989,97	400,76	8336,04
46	2,50%	3,66%	1,53%	0,29%	14 569 072,39	1051,34	1538,55	643,26
47	1,59%	-1,22%	1,52%	3,26%	89 040 683,89	46199,30	-35370,71	44192,29
48	2,32%	-2,38%	1,59%	0,88%	25 000 041,81	5075,95	-5210,13	3488,49
49	0,13%	-3,87%	1,62%	2,88%	17 673 224,83	674,68	-19718,88	8228,51
50	-1,17%	1,51%	0,31%	0,17%	5 375 072,49	-106,52	137,93	28,05
51	1,01%	0,67%	-0,18%	0,19%	4 700 199,73	89,66	58,83	-16,04
52	0,63%	-1,30%	-0,10%	0,19%	1 907 460,69	23,36	-48,18	-3,60
53	1,67%	1,51%	-1,03%	0,06%	3 985 400,31	39,47	35,64	-24,22
54	1,97%	1,84%	-0,39%	0,22%	7 447 977,04	320,97	299,63	-63,93
60	-0,14%	0,96%	-0,38%	0,30%	5 019 973,78	-20,27	143,87	-56,29
61	1,92%	8,07%	-0,61%	0,08%	2 097 878,81	32,14	135,12	-10,28
62	1,59%	5,48%	0,05%	0,20%	5 194 922,20	162,91	563,42	5,32
63	2,74%	0,60%	-0,34%	0,34%	2 711 768,29	251,58	55,42	-31,54
64	1,96%	1,33%	0,97%	0,26%	580 527,01	29,90	20,34	14,86
70	-1,80%	-0,30%	-0,72%	0,55%	8 937 517,84	-892,28	-146,70	-355,01
71	-4,67%	3,22%	-0,29%	0,33%	1 829 822,15	-283,29	195,27	-17,61
72	-0,65%	-4,71%	0,08%	0,66%	903 045,44	-38,77	-282,38	4,90

73	6,13%	4,38%	-3,69%	0,61%	3 792 942,38	1412,79	1008,78	-851,16
74	-1,90%	5,20%	5,59%	0,45%	2 044 023,78	-174,40	476,02	512,10
75	-0,05%	4,09%	0,00%	2,77%	11 693 922,84	-152,48	13235,43	12,08
76	0,78%	-1,09%	-0,09%	1,07%	1 796 719,08	150,44	-209,71	-16,62
77	1,09%	-1,56%	0,10%	0,35%	1 103 085,21	42,23	-60,27	3,73
78	3,27%	-0,99%	0,28%	0,78%	5 602 875,18	1433,62	-431,90	123,47
79	0,05%	7,72%	2,64%	1,25%	4 718 964,70	28,13	4566,82	1560,87
80	-4,97%	1,74%	-0,13%	19,40%	11 401 536,28	-109920,67	38514,22	-2876,08
81	-3,27%	-0,87%	-0,16%	1,98%	52 129 387,79	-33769,52	-8971,66	-1634,36
82	0,54%	-3,44%	-0,29%	8,19%	25 870 547,09	11418,09	-72926,01	-6251,62
83	-0,95%	0,37%	-0,07%	3,72%	12 122 808,10	-4274,38	1664,77	-333,78
84	2,70%	-0,95%	-0,26%	7,08%	12 568 098,21	24067,24	-8416,19	-2332,68
86	6,42%	0,81%	-0,05%	4,41%	21 644 520,99	61349,66	7783,34	-452,45
87	1,63%	4,18%	-0,11%	17,00%	6 774 300,91	18721,95	48109,86	-1257,13
88	-0,23%	-7,28%	-2,93%	4,03%	6 460 750,46	-599,00	-18953,99	-7635,82
89	4,47%	-2,73%	-0,05%	3,06%	6 400 056,95	8769,48	-5352,96	-94,38